**Microbial nitrilases: versatile, spiral forming, industrial enzymes**

| | |
|---|---|
| Journal: | *Applied Microbiology* |
| Manuscript ID: | JAM-2008-0805.R1 |
| Journal Name: | 1 Journal of Applied Microbiology - JAM |
| Manuscript Type: | JAM - Review |
| Date Submitted by the Author: | n/a |
| Complete List of Authors: | Thuku, Robert; University of Cape Town, Electron Microscope Unit<br>Brady, Dean; CSIR, Biosciences<br>Benedik, Michael; Texas A&M University, Biology<br>Sewell, Bryan; University of Cape Town, Electron Microscope Unit |
| Key Words: | Biotechnology, Molecular genetic, Enzyme activity, Protein Engineering, Structural Biology |
| | |

# Microbial nitrilases: versatile, spiral forming, industrial enzymes

R. Ndoria Thuku[1,4], Dean Brady[2], Michael J. Benedik[3] and B. Trevor Sewell[1,5]

[1]Electron Microscope Unit, University of Cape Town, South Africa.

[2]CSIR Biosciences, Modderfontein 1645, Private Bag X2, Johannesburg, South Africa

[3]Department of Biology, Texas A&M University, Texas, USA

[4]Department of Molecular and Cell Biology, University of Cape Town, South Africa

[5]Institute of Infectious Disease and Molecular Medicine, University of Cape Town, South Africa

Running title: The spiral forming nitrilase structures

Subdivision: Review

Corresponding author: B. Trevor Sewell

Electron Microscope Unit, University of Cape Town, Private Bag, Rondebosch 7700, South Africa.

Telephone: +27216502817

Fax: +27216891528

Email: trevor.sewell@uct.ac.za

Enzyme: EC 3.5.5.1 nitrilase

Keywords: nitrilase, oligomer, spiral enzymes, nitrilase superfamily, helical enzymes

Word Count: 15855

## 1. Summary

The nitrilases are enzymes that convert nitriles to the corresponding acid and ammonia. They are members of a superfamily, which includes amidases and occur in both prokaryotes and eukaryotes. The superfamily is characterized by having a homodimeric building block with a αββα-αββα sandwich fold and an active site containing four positionally conserved residues: cys, glu, glu and lys. Their high chemical specificity and frequent enantioselectivity makes them attractive biocatalysts for the production of fine chemicals and pharmaceutical intermediates. Nitrilases are also used in the treatment of toxic industrial effluent and cyanide remediation. The superfamily enzymes have been visualized as dimers, tetramers, hexamers, octamers, tetradecamers, octadecamers and variable length helices, but all nitrilase oligomers have the same basic dimer interface. Moreover, in the case of the octamers, tetradecamers, octadecamers and the helices, common principles of subunit association apply. While the range of industrially interesting reactions catalysed by this enzyme class continues to increase, research efforts are still hampered by the lack of a high resolution microbial nitrilase structure which can provide insights into their specificity, enantioselectivity and the mechanism of catalysis. This review provides an overview of the current progress in elucidation of structure and function in this enzyme class and emphasizes insights that may lead to further biotechnological applications.


## 2. Introduction

The nitrilases (EC 3.5.5.1) are an important class of industrial enzymes belonging to the nitrilase superfamily (Pace and Brenner, 2001), and are expressed widely in both prokaryotes and eukaryotes. Nitrilases hydrolyze various nitriles to the corresponding acid and ammonia, although they occasionally release an amide product (Fernandes et al., 2006). The nitrilase superfamily comprises thirteen different enzyme classes that share significant structural homology despite varying sequence conservation. In general, the superfamily members include the microbial nitrilases (nitrilases, cyanide dihydratases and cyanide hydratases), aliphatic amidases, amidohydrolases and acyl transferases of differing specificities (Brenner, 2002). The majority of the known enzymes were obtained from bacteria, fungi and plants by a variety of selection methods on media containing nitriles as nitrogen sources (O'Reilly and Turner, 2003; Martinkova et al., 2008) or through direct cloning and expression. Although the physiological role of nitrilases is still not clear, they may play a variety of diverse roles in the cell. The production of metabolites is exemplified by the synthesis of indole acetic acid (Bartel and Fink, 1994; Bartling et al., 1992, 1994), whereas their role in detoxification has been shown for

cyanide in plants (Piotrowski et al., 2001), the degradation of glucosinolates (Bestwick et al. 1993), and the aldoxime degrading pathway (Kato et al. 2000).

Some information regarding their natural role can be surmised from studying the control of nitrilase gene expression. While bacteria such as *Bacillus subtilis* ZJB-063, constitutively express nitrilases (Zheng et al., 2007), the majority of the characterized nitrilases are inducible by the presence of nitriles in the growth media (Banerjee et al., 2002) which would seem to indicate that they play a role in detoxification or utilization. In a variety of fungi, expression of the cyanide degrading nitrilase is specifically induced by the presence of cyanide in the growth medium. In contrast, the expression of the CynD from *B. pumilus* was not found to be regulated by cyanide, but is controlled by the sporulation cascade. It is induced by $Mn^{2+}$ (Meyers et al., 1993), a well-known inducer of sporulation, and is abolished in *spoOA* mutants. CynD has not been specifically linked to any biological role in bacteria, but nonetheless has been exploited for biotechnological purposes.

In seven classes of the nitrilase superfamily, the nitrilase domain is fused to another domain (Brenner, 2002). One such case is the $NAD^+$ synthetase from *Mycobacterium tuberculosis* (Bellinzoni et al., 2005). This enzyme relies on an associated amino-terminal amidase domain in order to utilize glutamine as a source of nitrogen and liberate ammonia which is required for the synthesis of $NAD^+$. The inactivation of the amidase domain by mutation of the catalytic cysteine inactivated the associated $NAD^+$ synthetase, and suggested that $NAD^+$ synthetase is a potential drug target (Bellinzoni et al., 2004). Nitrilases are attractive biocatalysts in the fine chemicals and pharmaceutical industry because of their high specificity and chemo-, regio- and enantio-selectivity (Brady et al., 2004). They are also used in the detoxification of industrial waste and herbicide degradation (Banerjee at al., 2002). In general, the nitrile biocatalysts operate in aqueous solutions at moderate temperatures and pH, and this minimizes the costs of chemical processes and the negative impact of industry on the environment (Singh et al., 2006; Brady et al., 2006).

There are over 200 known nitrilase sequences (Robertson et al., 2004). A recent study identified nitrile-hydrolyzing activities in 40 distinct species of bacterial and yeast isolates (Brady et al., 2006). While our knowledge of their sequence information, environmental distribution and substrate specificity continues to increase, the crystal structure of a microbial nitrilase remains elusive. Consequently, the lack of specific structural information on these enzymes hinders the correlation of sequence, activity and specificity (Podar et al., 2005).

Nevertheless, there are eleven atomic structures of distant homologous enzymes in the nitrilase superfamily which provide key insights into the enzyme structure. These include the Nit domain of the NitFhit fusion protein (PDB code 1ems), three N-carbamoyl-D-amino acid amidohydrolases from *Agrobacterium* sp. Strain KNK712 and *Agrobacterium radiobacter* (PDB codes 1erz, 1fo6 and 1uf5), the putative CN hydrolase from yeast (PDB code 1f89), the hypothetical protein PH0642 from *Pyrococcus horikoshii* (PDB code 1j31), XC1258, a putative prokaryotic Nit protein from *Xanthomonas campestris* (PDB code 2e11), the β-alanine synthase from *Drosophila melanogaster* (PDB code 2vhi and 2vhh), the AmiF formamidase from *Helicobacter pylori* (PDB codes 2dyu, 2e2k and 2e2l), and two aliphatic amidases from *Pseudomonas aeruginosa* and *Geobacillus pallidus* RAPc8 (PDB codes 2uxy and 2plq, respectively) (Pace et al., 2000; Nakai et al., 2000; Wang et al., 2001; Hashimoto et al., 2004; Kumaran et al., 2003; Sakai et al., 2004; Chin et al., 2007; Lundgren et al., 2008; Hung et al., 2007; Andrade et al., 2007 and Kimani et al., 2007, respectively). Despite varying sequence identity (~20%), all the structures share a characteristic monomer fold and conserve two glutamates, lysine and cysteine in their catalytic site. The monomers associate in a common manner to form an αββα-αββα sandwich.

The microbial nitrilases have been shown to form homo-oligomeric spirals using a combination of negative stain electron microscopy and the docking of homology models (Sewell et al., 2003; Thuku et al., 2007; Woodward et al., 2008; Dent et al., 2008; Vejvoda et al., 2008). The best characterized enzyme is the nitrilase from *Rhodococcus rhodochrous* J1 which is capable of converting acrylonitrile and 3-cyanopyridine to acrylic acid and nicotinic acid, respectively (Kobayashi et al., 1988, Mathew et al., 1988). This enzyme exists as an inactive dimer which oligomerizes to form active spirals in the presence of benzonitrile or an autolytic cleavage of the C-terminus (Nagasawa et al., 2000, Thuku et al, 2007). This phenomenon has most frequently been described in those nitrilases arising from the genus *Rhodococcus* (Harper, 1977b, 1985; Hoyle et al., 1988; Stevenson et al., 1992). The monomer association occurs via two interfaces, namely the 'A' and 'C' surfaces and forms a one-start, left-handed spiral (Sewell et al., 2003). The modification of residues within these surfaces inactivates the enzyme and possibly suggests that a link exists between oligomerization at these surfaces and the active site (Sewell et al., 2005). In order to fully understand the spiral structures, it is therefore necessary to characterize these interfaces and their mechanism of activation.

In this review, we describe the structural insights we have gained from studying the nitrilase from *Rhodococcus rhodochrous* J1 and other closely related enzymes, namely the cyanide dihydratases, the cyanide hydratases and an amidase. We also incorporate structural insights from other nitrilase homologues whose structures have been determined at atomic resolution. Further biotechnological advances involving these enzymes make it important to expand on their structure, the details of the interacting surfaces, and their reaction mechanism. This will lead to the development of improved biocatalysts (more stable, specific and versatile enzymes) and additional processes using nitrile-hydrolyzing enzymes.

## 3. Enzyme structure and homology

The microbial nitrilases are generally known to exist as inactive dimers in solution except the active dimeric enzyme from *Pyrococcus abyssi* (Mueller et al., 2006). The majority of these enzymes have a subunit size of between 30-45 kDa (Banerjee et al., 2002; O'Reilly and Turner, 2003), which self associate to form active oligomers having between 4 – 22 subunits (Table 1), or active spirals of variable length (Sewell et al., 2005; Thuku et al., 2007; Woodward et al., 2008; Vejvoda et al., 2008; Dent et al., 2008). The exceptions include the 76 kDa nitrilase from *Fusarium solani* (Harper, 1977a), and the monomeric enzymes from *Arthrobacter* sp. strain J1 (Bandyopadhyay et al., 1986) and *Rhodococcus rhodochrous* PA-34 (Bhalla et al., 1992). However, as none of these atypical nitrilases have been sequenced, their homology to the nitrilase superfamily enzymes remains unknown. The molecular mass of the enzyme subunit and the active complex is usually determined in the absence of the substrate by size exclusion chromatography, native- and SDS-PAGE, mass spectroscopy, light scattering and electron microscopy.

Despite varying sequence conservation and differing substrate affinities, all the superfamily enzymes demonstrate significant structural homology and can be aligned with the crystal structures of 1ems, 1erz, 1uf5, 1fo6, 1f89, 1j31, 2e11, 2vhi, 2plq, 2dyu and 2uxy using a program such as mGenTHREADER (Jones, 1999; McGuffin and Jones, 2003). Each enzyme monomer has an αββα-fold which associates to form an 8-layered αββα-αββα dimer (Figure 1) across the 'A' surface (Sewell et al., 2003). While the solved structures form dimers, tetramers, hexamers or octamers, the microbial nitrilases form larger homo-oligomeric spirals with a varying number of subunits. The dimer is the primary building block for oligomerization and their association occurs in a variety of ways among the superfamily enzymes. In particular, the Rhodococcal nitrilases (Harper 1977b, 1985; Stevenson et al., 1992; Nagawasa et al.; 2000)

could form a complex estimated at having 10-12 subunits in the presence of substrate, on heat treatment, or addition of ammonium sulphate or organic solvent. We recently reported a long regular helix of the nitrilase from *R. rhodochrous* J1 in which the short active 'c' shaped oligomers undergo an autolysis removing 39 C-terminal amino acids and causing them to form long regular helices (Thuku et al., 2007). Active 'c' shaped homo-octamers (Figure 2) which appear superficially similar have recently been visualized at atomic resolution in the nitrilase-related β-alanine synthase from *Drosophila melanogaster* (Lundgren et al., 2008). This enzyme catalyzes the removal of the N-carbamyl group of N-carbamyl-β-alanine and N-carbamyl-β-aminoisobutyrate to form β-alanine and β-aminoisobutyrate, respectively, with the release of carbon dioxide and ammonia (Schnackerz and Dobritzsch, 2008). The correlation of the shape of the fruit fly enzyme to the 'c' shape of the *R. rhodochrous* J1 nitrilase oligomers (Thuku et al., 2007) and the fact that there are approximately 10 subunits per turn of helix, suggests that the *Rhodococcal* enzyme could also form an octamer.

The cyanide dihydratase from *B. pumilus* C1 was also found as both a short spiral and a long helix but differed in that it showed a reversible pH-dependent switching between an 18-subunit terminating spiral to a variable length helix (Jandhyala et al., 2003) at pH5.4. Other known spiral structures include the 14-subunit self-terminating cyanide dihydratase from *P. stutzeri* AK61 (Sewell et al., 2003), and the long regular helices of the cyanide hydratases from *G. sorghi* (Woodward et al., 2008) and *N. crassa* (Dent et al., 2008), and the nitrilase from *Aspergillus niger* K10 (Vejvoda et al., 2008).

There are numerous suggestions of the functional significance of the oligomerization. Jandhyala et al (2005) observed an increase in activity relative to a homologue in which the pH dependent switching does not occur at the pH at which the size of the cyanide dihydratase increased in the *B. pumilus* C1. The increase in activity accompanying an increase in complex size is commonly observed in Rhodococcal species where inactive dimers and active higher oligomers are found (Harper 1977b, 1985; Nagasawa et al., 2000; Stevenson et al., 1992). The functional complexity of subunit association is nowhere better illustrated than in the case of the plant nitrilases which are known to possess two or three nitrilase isoforms in their tissues. Recent reports suggest that these enzymes could either have a dual biological function or broaden their substrate spectrum through the formation of higher heteromeric complexes (Jenrich et al., 2007; Kriechbaumer et al., 2007). In particular, the *Zm*Nit1 and *Zm*Nit2 nitrilases from maize were observed to form a complex that could synthesize auxin (indole-3-

acetic acid) as well as hydrolyse β-cyanoalanine, an intermediate in cyanide detoxification (Kriechbaumer et al., 2007). In the plant *Sorghum bicolor*, the individual nitrilase isoforms are inactive but upon heteromeric assembly, they acquired activity and could hydrolyse β-cyanoalanine and other substrates (Jenrich et al., 2007).

Multiple alignments of the helix or spiral forming nitrilase sequences showed that these proteins have two significant insertions (12-16 amino acids) in their sequences and an extended C-terminus (Figure 3) relative to the sequences of the first two crystallographically determined structures (1erz and 1ems). Because of the multiple forms of association of the nitrilase monomers, it was necessary to label the areas of association. The residue insertions correspond to the 'C' surface and this is required to form the one-start left-handed spiral (Sewell et al., 2003). It has been shown that the modification of the residues in the 'C' surface by mutation destroyed the activity of the cyanide dihydratases from *B. pumilus* C1 and *P. stutzeri* AK61 (Sewell et al., 2005). As seen in Figure 1, all superfamily enzymes conserve the catalytic residues, namely a glutamic acid, a lysine and a cysteine in the active site (Brenner, 2002). In addition, a glutamic acid (corresponding to glu 142 in the *G. pallidus* amidase structure), which has been implicated in the nitrilase reaction mechanism is also highly conserved (Kimani et al., 2007). It is interesting that apart from the active site residues, only four glycines are absolutely conserved throughout the known superfamily sequences.

The docking of a homology model of the *P. stutzeri* AK61 enzyme into the negative stain density of its spiral structure located the extended C-terminal tail facing the center of the spiral (Sewell et al., 2003). This situation is similar to that of the crystalline β-alanine synthase (Lundgren et al., 2008), but different in the homologous crystalline amidases which have D3 symmetry and in which the C-terminal tail is located on the outside of the hexamer (Andrade et al., 2007; Hung et al., 2007; Kimani et al., 2007). In the majority of the nitrilase atomic homologues, this part of the molecule is seen to interact at the 'A' surface with its equivalent from another monomer. Even though the aliphatic amidases have an extended C-terminal tail similar to that of the microbial nitrilases, the lack of sequence and structural homology suggests there is high variability in this region. We have previously shown that the docking of homology models in the three-dimensional reconstructions of these enzymes, can provide a framework by which the basis for oligomerization and stabilization can be explained (Sewell et al., 2003; Thuku et al., 2007; Woodward et al., 2008; Dent et al., 2008). In addition, the

alignment presented in Figure 3 provides a basis for homology modeling from which the enzyme structure and the identification of the interfacial residues can be inferred.

## 4. Substrate specificity

The nitrilases have previously been classified on the basis of their substrate affinity (Kobayashi and Shimizu, 1994; Banerjee et al., 2002; O'Reilly and Turner, 2003). While most nitrilases are specific for aromatic nitriles, others have preference for only arylacetonitriles, aliphatic nitriles, bromoxynil or cyanide. We continue to use this broad classification of the biochemically characterized nitrilases and highlight their physical properties, substrate specificity and activity in Table 1 even though there are examples of enzymes that fall into two different categories, for instance arylacetonitrilases that convert aliphatic substrates (Heinemann et al., 2003).

The aromatic nitrilases are highly specific for aromatic and heterocyclic nitriles. The best characterized enzyme is the nitrilase from *Rhodococcus rhodochrous* J1 (Kobayashi et al., 1989). However, there is a degree of flexibility in the nitrilase substrate range. For instance, the enzymes from *R. rhodochrous* J1 and *Rhodococcus* (formerly *Nocardia*) NCIMB 11216 could hydrolyse acrylonitrile and propionitrile respectively, following activation in the presence of benzonitrile (Nagasawa et al., 2000; Hoyle et al., 1998). Recent reports suggest that the occurrence of aromatic nitrilases in filamentous fungi is common (Kato et al., 2000; Kaplan et al 2006a-c; Vejvoda et al., 2006a-b). Four aromatic fungal nitrilases have been characterized to date, namely those from *Fusarium solani* IMI196840, *Fusarium oxysporum* f.sp. *melonis*, *Aspergillus niger* K10 and *Fusarium solani* O1 (Harper, 1977; Goldlust and Bohak, 1989; Kaplan et al., 2006c; Vejvoda et al., 2008, respectively). These enzymes share high specificity for aromatic substrates and good thermostability. The enzymes from *A. niger* K10 and *F. solani* O1 were shown by electron microscopy (Vejvoda et al., 2008) to form spiral structures similar to those previously reported (Sewell et al., 2005; Thuku et al., 2007).

Although aliphatic nitrilases are capable of hydrolyzing benzonitrile, the rate of hydrolysis is highest with the aliphatic nitriles. In general, these enzymes occur in plants and bacteria (Table 1). There are several reports of homologous nitrilases in plants (Dohmoto et al., 1999, 2000; Park et al., 2003), however, the *At*NIT1 enzyme is the only biochemically characterized plant nitrilase to date. The recombinant NIT1 nitrilase from *Arabidopsis thaliana* (*At*NIT1) had 270

times more activity with 3-phenylpropionitrile than that observed with benzonitrile (Osswald et al., 2002).

The heterologous expression of bacterial nitrilases in plants has also been achieved. The nitrilase of *Klebsiella pneumoniae* subsp. *ozaenae* is highly specific for the herbicide bromoxynil (3,5-dibromo-4-hydroxybenzonitrile). The native and recombinant enzymes completely converted bromoxynil to the acid which enabled the bacterium to use the liberated ammonia as the sole source of nitrogen (McBride et al., 1986; Stalker et al., 1988a). This enzyme was observed to be active *in vitro* as a dimer and showed no activity with benzonitrile (Stalker et al., 1988a). The incorporation of the bacterial gene (*bxn*) encoding the bromoxynil-specific nitrilase into the leaves of transgenic tobacco plants was reported to confer resistance to high levels of the herbicide Buctril® (or commercial bromoxynil) (Stalker et al., 1988b). The bacterial gene was spliced to plant-promoters and the genes expressing the bromoxynil-specific nitrilase were introduced into cotton varieties via *Agrobacterium* transformation with the same effects (Stalker et al., 1996). This discovery has led to the development of Bromoxynil-resistant cotton (BXN$^{TM}$) which is widely grown in the USA and indeed, this represents one of the most successful biotechnological applications of a nitrilase.

The arylacetonitrilases are generally enantioselective enzymes that display activity with benzonitrile and sometimes the aliphatic nitriles. In particular, the native and recombinantly purified enzymes from *Pseudomonas fluorescens* EBC191 could convert 2-acetoxybutenenitrile to the corresponding acid with higher specificity than the enzyme from *Synechocystis* spp. 6803, an aliphatic nitrilase (Heinemann et al., 2003). These observations suggest that the substrate specificities of the microbial nitrilases is wider than is generally assumed. The nitrilases from *Alcaligenes faecalis* ATCC 8750 (Yamamoto et al., 1991) and *P. fluorescens* EBC191 (Kiziak et al., 2005) could convert (R,S)-mandelonitrile to (R)-(-)mandelic acid, an important intermediate in the pharmaceutical industry. While the majority of the arylacetonitrilases could hydrolyse mandelonitrile at a lower rate compared to that of phenylacetonitrile, the mandelonitrile hydrolase from *Bradyrhizobium japonicus* USDA110 is highly specific for mandelonitrile (Zhu et al., 2007, 2008). The mandelonitrile hydrolase genes have been found to occur on the same operon that encodes other enzymes involved in the mandelonitrile metabolic pathway. For this reason, it was suggested that these enzymes could play a role in the detoxification of harmful nitriles during the metabolism of cyanogenic glycosides (Kiziak et al., 2005; Zhu et al., 2007).

The cyanide dihydratases and cyanide hydratases catalyze the hydrolysis of cyanide (HCN) with high specificity to formate and formamide, respectively. In particular, the cyanide hydratase from the fungus *Fusarium lateritium* had a 3000-fold higher activity towards KCN compared to benzonitrile (Nolan et al., 2003). The cyanide dihydratases occur mostly in bacteria whereas the cyanide hydratases occur in filamentous fungi (O'Reilly and Turner, 2003). The structures of the enzymes from *B. pumilus*, *P. stutzeri* AK61, *N. crassa* and *G. sorghi* are spirals which conserve the oligomeric principles previously reported (Sewell et al., 2005). While the details of the mechanism of cyanide degradation are not clear, it was proposed that subtle differences in the active site configuration of these enzymes dictate whether ammonia or formamide is the better leaving group (Jandhyala et al., 2005). The fungal cyanide hydratases have been shown to be capable of degrading metal cyanides and these enzymes could have potential applications in the treatment of waste from the metal plating industry (Yanase et al., 2000; Barclay et al., 1998). However, the microbial treatment of toxic industrial effluent is often hindered by varying levels of pH and temperature which often inhibits microbial growth (Baxter and Cummings, 2006). Nevertheless, the potential exists for re-engineering these enzymes to tolerate harsh reaction conditions and use them for on-site cyanide remediation (Jandhyala et al., 2003). Mutants of *B. pumilus* with improved pH tolerance have been identified. However substrate inhibition remains a problem with these enzymes and this limits their industrial application under conditions where high substrate concentrations would occur.

In general, the natural substrates for the majority of the nitrilases are not known. Structural and modeling studies in other homologous superfamily enzymes, namely DCase from *Agrobacterium* sp (Nakai et al., 2000; Chen et al., 2003; Hashimoto et al., 2004), the CN hydrolase from yeast (Kumaran et al., 2003), and several aliphatic amidases (Andrade et al., 2007; Hung et al., 2007; Kimani et al., 2007) with bound substrates have suggested that the residues lining the active site cavity and the volume of the cavity determine the type and size of substrate that is hydrolysed. Kimani et al. (2007) also suggested that the enantioselective properties for the D- and not the L-enantiomer of lactamide in the enzyme from *G. pallidus* RAPc8 was due to the steric clash between the L-lactamide hydroxyl group and the glu142 carboxylate. Some insights into the specificity of the amidases, which provide an explanation for the results of Karmali et al. (2001) and Makhongela et al. (2007), were derived from the crystal structures. The location of Trp138, obstructing the opening of the active site, explains

the normal preference for small substrates and explains why its mutation to a glycine allows hydrolysis of phenylamide and *p*-nitrophenylamide. Clearly, the insights from the nitrilase homologous structures can be applied in the modeling of the substrate preference and the enantioselectivity of the microbial nitrilases.

## 5. Enzyme engineering

The creation of enzymes catalyzing reactions of use for industrial applications has been successful with nitrilases. Insight into the determinants of substrate specificity or activity of the nitrilases has been obtained through an analysis of random mutagenesis studies (Table 2) in which modification of specific residues has changed either the substrate profile or the activity. At present, the structural reason for the activity changes can only be inferred from the study of nitrilase homologues, in particular the DCase and the amidases. For example, in the aliphatic amidase from *Pseudomonas aeruginosa*, the modification of tryptophan 138 (which is located in the substrate binding pocket) to glycine allowed this enzyme to act on aliphatic and aromatic amides (Karmali et al., 2001). This residue is structurally conserved in the other aliphatic amidases whose structures have been determined. The mutant W138G allowed the hydrolysis of bulky aromatic substrates such as phenylacetamide and *p*-nitrophenylacetamide. In the *R. rhodochrous* J1 nitrilase, a threonine occurs at the equivalent position suggesting that a modification of substrate specificity could be achieved in the microbial enzymes.

Gene site saturation mutagenesis (a high throughput screening technique in which all possible point mutations are explored) was applied by DeSantis et al (2002, 2003) to an aliphatic nitrilase isolated from the environment. This resulted in an improved enzyme that could hydrolyse 3-hydroxyglutaryl nitrile to (R)-4-cyano-3-hydroxybutyric acid, an important pharmaceutical intermediate for synthesis of the cholesterol-lowering drug Avorastatin (Lipitor). In particular, a single residue change (alanine 190) to histidine, threonine or serine resulted in an enzyme that could convert the substrate at high concentrations to the (R)-acid with a higher enantiomeric excess than the wild type enzyme. The “enantio-selectivity hot-spots” at 190 and 191 are situated in the loop between β8 and α6. This region is difficult to model based on known homologous structures but probably forms a side of the opening to the active site. Similarly, the enzyme from *Acidovorax facilis* 72W has recently been engineered for the commercial production of 3-hydroxyvaleric acid (Wu et al., 2007) and glycolic acid (Panova et al., 2007; Wu et al., 2008), using selected mutagenesis, over-expression in *E. coli* and the immobilization of whole cells in recyclable beads. The specific activity of the mutants

T210A and F168V/L201N clones was approximately 7- and 15-fold higher, respectively, compared to the wild-type enzyme. On the basis of structural alignment, the modified residues are located in the α6 helix (threonine 210), substrate binding pocket and close to active site cysteine (phenylalanine 168), and in the loop between strand β8 and α6 helix (leucine 201). It is not structurally clear why these modifications resulted in a significantly improved biocatalyst. We speculate that the increased activity per cell of the recombinant enzyme (that is, 125-fold higher than the native organism) is mostly due to over-expression.

## 6. The reaction mechanism

All the superfamily enzymes conserve the three catalytic residues, namely a cysteine which acts as a nucleophile, a glutamate that acts as a general base catalyst and a lysine which stabilizes the tetrahedral intermediate (Brenner, 2002; Wang et al., 2001; Andrade et al., 2007; Hung et al., 2007; Nakai et al., 2000). While the nitrilase reaction mechanism is not well defined, considerable information can be inferred from structural studies of other members of the superfamily, in particular DCase and amidase. Structures of mutants of both of these enzymes in which the active site cysteine has been modified (Chen et al., 2003; Hung et al., 2007) have enabled the visualization of the bound substrate. In both these enzymes, the amide nitrogen of the substrate is within hydrogen bonding distance of two glutamates in the active site (47 and 146 in DCase). The positions of both of these glutamates are conserved in the known structures and it has been suggested that these interactions play an important role in positioning the substrate. It is thought that the active site cysteine initiates a nucleophilic attack on the substrate to form a tetrahedral intermediate as originally proposed by Stevenson et al (1992). One of the two glutamates (Glu47) increases the nucleophilicity of the cysteine and participates in the proton transfer giving rise to ammonia. The tetrahedral intermediate is thought to be stabilized by the conserved lysine and by the backbone amino group of the residue following the cysteine in the case of the amidase. The thioester intermediate formed after the release of the ammonia then undergoes a general base catalysed nucleophilic attack by a water forming a second stabilized tetrahedral intermediate. This tetrahedral intermediate formed following nucleophilic attack on an acetyl intermediate by hydroxylamine has actually been visualized (Andrade et al, 2007). The tetrahedral intermediate then breaks down with the release of the acid product (in the case of hydrolysis) and the restoration of the enzyme.

The observation that the acyl intermediate would prevent access of a water to the vicinity of the primary active site glutamate (E59 in the *Geobacillus pallidus* amidase) led to the suggestion

that the hydrolysis could be catalysed by the second glutamate residue (E142 in the *Geobacillus pallidus* amidase) whose side chain is in a suitable position to act as the general base catalyst (Kimani et al, 2007). It has been observed that the *G. pallidus* amidase E142L mutant is inactive and leads to the formation of a covalently modified cysteine with certain substrates (Brandon Weber*, personal communication*). Furthermore, the location of E142 on a loop which in the nitrilases is directed into the 'C' surface, has led to the suggestion that the residue is moved into position by oligomerization (Kimani et al., 2007), and therefore explains the inactivity of nitrilase dimers, particularly in the well characterized *Rhodococcal* nitrilases.

It is suggested (Brenner, 2002; Jandhyala et al., 2005) that in the case of a nitrile substrate, a thioimidate is formed after the first nucleophilic attack which is then hydrolysed with the release of ammonia and an acyl intermediate in the case of the nitrilases and the cyanide dihydratases, or formamide in the case of the cyanide hydratases. In the former case, the acyl intermediate is then subjected to a second hydrolysis step which is similar to that postulated for the amidases and DCases. As seen in Table 1, some significant amide concentration is detected among the nitrilase-catalyzed reaction products, suggesting that the scissile bond in the thioimidate tetrahedral intermediate is not well determined for these substrates. The plant nitrilases, in particular, produce a high proportion of amide by-product (Hook and Robinson, 1964; Robinson and Hook, 1964; Effenberger and Osswald, 2001; Osswald et al., 2002; Piotrowski et al., 2001). In addition, Kiziak et al (2005) reported amide formation for the arylacetonitrilase from *Pseudomonas fluorescens* EBC191 in the range 8-89% depending on substrate. In this enzyme, a positive correlation was observed between the amount of amide produced and the electron-deficiency of the α-substituent (Fernandes et al., 2006), suggesting a subtle interaction between the active site and substrate.

An interesting question is what distinguishes an enzyme having nitrilase activity from one having amidase activity but since no active nitrilase structures have been solved the question remains unanswered. A close homologue of the *Pyrococcus horikoshii* enzyme (1j31) has been observed to have activity on fumaronitrile and malononitrile (Mueller et al., 2006) and this suggests a possible fruitful area for future research.

## 7. Spiral formation among microbial nitrilases

All the nitrilases, cyanide dihydratases and cyanide hydratases studied by us (Figure 3) form a spiral quaternary structure. While some of these enzymes form helices of variable length,

others form short, terminating spirals which have a specific number of subunits (Figure 4). In particular, the cyanide dihydratase from *P.stutzeri* AK61 forms a 14-subunit spiral (Sewell et al., 2003), whereas the homologous enzyme from *B. pumilus* C1 and 8A3, form an 18- and a 22-subunit spiral, respectively (Jandhyala et al., 2003; Johann Eicher, *personal communication*). The nitrilases from *Rhodococcus rhodochrous* J1 (Thuku et al., 2007) and *Fusarium solani* O1 (Vejvoda et al., 2008), are also seen as short spirals by electron microscopy, however, the exact number of subunits is yet to be determined. The cyanide hydratase enzymes from *G. sorghi* (Woodward et al., 2008), *N. crassa* (Dent et al., 2008) and *A. niger* K10 (Vejvoda et al., 2008), occur as long, variable length helices.

There is growing evidence that the principles governing the association of monomers to form oligomers (Sewell et al., 2005) are common among this class of enzymes. As seen in Figure 4, the shape of the density which encloses the dimer, the conserved dyadic axes and the connectivity between the dimers which extends the assembly can be clearly discerned. The spiral oligomers are generally left-handed following handedness determination in other homologous enzymes (Jandhyala et al. 2003; Woodward et al., 2008). In addition, the homo-octameric spiral of the homologous, crystallized fruit fly beta alanine synthase is left-handed (Lundgren et al., 2008). Structural studies involving three-dimensional reconstruction and modeling based on the available nitrilase atomic homologues have enabled the identification of interacting regions between the subunits, which have been labeled ‘A’, ‘B’, ‘C’, ‘D’, ‘E’ and ‘F’ surfaces (Figure 4). The ‘A’, ‘C’, ‘D’ and ‘F’ surfaces are related by two-fold axes whereas the ‘E’ surface is asymmetric. Even though these regions of interactions appear to be common, the association of subunits at the different interfaces leads to the variety of oligomeric shapes that are seen in these enzymes. While the ‘A’, ‘C’, ‘D’ and ‘F’ surfaces participate in spiral formation, the ‘B’ surface does not. This surface occurs only in three crystal forms, namely the NitFhit protein (Pace et al., 2000), N-carbamyl-D-amino acid amidohydrolase (DCase, Nakai et al., 2000) and the prokaryotic XC1258 Nit protein (Chin et al., 2007), in which the subunits form tetramers with 222 point group symmetry. Use of the ‘B’ surface results in a closed point group and the basis of these interactions is hydrogen bonding along the exposed side of a beta sheet between subunits. On the basis of sequence alignment, model building and three-dimensional electron microscopy, it can be inferred that the interactions at the surfaces are generally electrostatic. The only surfaces that have been visualized at atomic resolution in the nitrilase homologues are the ‘A’ and ‘C’ surfaces. Details of other surfaces arise from docking

of homology models into their three-dimensional electron microscopic reconstructions and must therefore be regarded as suggestions until they are verified by mutational analysis.

### 7.1 The 'A' surface

The association at the 'A' surface, involving helices α5 and α6, occurs in all crystalline and spiral structures. The surface has been frequently visualized at atomic resolution and the interactions across this surface are the basis for dimerization. The details of the intermolecular salt bridges and hydrophobic interactions in the high resolution structures vary. Thus, for example, in the *G. pallidus* amidase, interactions in α6 comprise a series of interdigitated methionines (M202, M203 and M207) and α5 has a pair of salt bridges formed by E173 and R176, in the case of NitFhit there are salt bridges in α6 between R211 and E214, in the *Pyrococcus* hypothetical protein (1j31) there are salt bridges between both α5 (E153 and R156) and α6 (R184 and E187) ( all the salt bridges are highlighted in Figure 3) and in DCase the 336 intersubunit interactions are mostly hydrophobic (Wang et al., 2001). In the prokaryotic XC1258 Nit protein (Chin et al., 2007), the α5 helix is slightly longer. An inspection of the sequences in the α5 and α6 helices of the spiral forming enzymes shows there is possible substitution of the salt bridges with hydrophobic residues. This situation is not yet clear due to lack of atomic detail in these enzymes. Additional structural elements sometimes interact across the 'A' surface and 'strengthen' it. In the *G. pallidus* amidase, a region of the C-terminal tail comprising four helices (α8, α9, α10 and α11) form an 'interlock' with the equivalent region from the two-fold related monomer (Kimani et al., 2007). There is considerable sequence and structural variability in the tail region and generalization about the details is not possible, however, interactions in the tail which contribute to the 'A' surface do occur in all the known structures where the tail exists. In the case of the β-alanine synthase from *D. melanogaster* (Lundgren et al., 2008), the 'A' surface is strengthened by interactions between the two additional N-terminal helices and a pair of C-terminal helices similar to those seen in the crystalline amidases (α9). In addition, the carboxy-terminal end of the tightly associated dimer is held in place by a parallel interaction between a pair of strands, one located in the tail region (β16) and the other on the surface of the partner subunit (β9). In general, the interactions at the 'A' surface not only hold the subunits together, but are also necessary for positioning the catalytic cysteine residue within the active site pocket. This residue is located on a $3_{10}$ helix which is part of the β-strand-turn-helix structural motif referred to as the 'nucleophilic elbow' (Kumaran et al., 2003). This motif is generally conserved in all the superfamily enzymes and is formed by the strand β7 and the α5 helix. This also provides an explanation for the loss of

activity that was reported in these enzymes after modification of the interfacial residues (Sewell et al., 2005). Although the structural elements at the interface appear to be common in the solved structures, there is very little sequence conservation either in the interacting helices or in the linking regions.

### 7.2 The 'C' surface

The association at the 'C' surface is the key to the formation of the spiral quaternary structures. It is located approximately at right angles to the 'A' surface and thus it is easy to see how the association at the 'A' and 'C' surfaces leads to an extended assembly. The details of the angular relationship between the two surfaces clearly determine the nature of the spiral which the extended assembly will form. As seen in Figure 3, there is no obvious conservation of amino acids occurring in this region. There is some evidence of conformational flexibility in this region from the structures of the fungal cyanide hydratases (Dent et al., 2008a; Woodward et al., 2008), the fruit fly β-alanine synthase (Lundgren et al., 2008) and several aliphatic amidases (Andrade et al., 2007; Hung et al., 2007; Kimani et al., 2007), which leads to a variety of oligomeric structures. When homology models are fitted into the low-resolution spiral structures, there is some vacant density visible at the 'C' surface which suggests these residues are absent in the solved structures (Figure 5, Thuku et al., 2007). The two insertions commonly occurring in the α2 helix and the beta bend between β10 and β11 are strongly implicated in this region. Predictions of secondary structure using PSIPRED (Bryson et al., 2005) showed that the residues inserted at α2 simply extend the helix in its amino-terminal while those located in the bend between β10 and β11 form a coil which makes it difficult to make a reasonable statement about the path of these residues or their possible contribution in the 'C' surface. The first detailed visualization of the 'C' surface has come recently from the crystal structure of the β-alanine synthase from *Drosophila melanogaster* (Lundgren et al., 2008), which clearly identifies the the major contributors to this surface that arise from three loop regions in each subunit, namely the residues between β2 and α2, β5 and α6, and β10 and β11, respectively. In particular, the residues between β10 and β11 in each subunit are seen to extend into a long coil which runs approximately at right angles to the 'A' surface, and interacts across the interface via two, symmetric salt bridges (E298 and K306). This region is disordered in the terminal subunits and was suggested to cause the octameric spiral assembly to terminate (Lundgren et al., 2008). Interestingly, charged residues are present in the region between β10 and β11 in the microbial spiral or helix forming enzymes, but not in identical locations according to our alignment. Nevertheless, the structure of the fruit fly beta alanine

synthase provides a basis for modeling these residue insertions in the microbial nitrilases and the structural alignment (Figure 3) can be used to design experiments which explore interacting residues in this region. The interactions in this region are both electrostatic and hydrophobic and between residues which are mostly buried. Apart from the residue insertions, there is involvement of other residues arising from different parts of the molecule which possibly confer stability to the 'C' surface (Lundgren et al., 2008). Similarly, the docking in the helical structure of the *Rhodococcus rhodochrous* nitrilase places an aspartate (residue 108) located in the bend between beta sheets β3 and β4 in close proximity to a lysine (residue 289) located on α7 suggesting the possibility of a stabilizing interaction across the interface (Thuku et al., 2007). The disruption of this surface by mutation abolished the activity in the cyanide dihydratases (Sewell et al., 2005). Therefore, a study of this region will definitely reveal how steric changes are transmitted to the active site so that the enzyme is activated.

### 7.3 The 'D' and 'F' surfaces

The 'D' surface association occurs only when the spiral completes one turn. The interactions at this surface occur across the groove of the spiral or helix (Figure 4 and 5). The docking of homology models into the spiral structures unambiguously locates the helices α1 and α3 in this region (Sewell et al., 2003). These two long helices are located on the same two-fold axis as the 'C' surface but on the opposite side of the spiral. An interesting feature of the helices in this region is that they comprise a mixture of positively and negatively charged residues, and we postulate that two-fold symmetric, electrostatic interactions maintain the elongating assembly (Sewell et al., 2005; Thuku et al., 2007). The location of charged residues in the 'D' surface is generally not conserved (Figure 3), and mutating much of the region made little difference to activity in the case of the cyanide dihydratases (Sewell et al., 2005). Interestingly, crystal packing interactions in the *G. pallidus* amidase structure (Kimani et al., 2007) involve residues K36 in α1 and E82 in α3 helices, which interact across a two-fold axis. A further stabilizing two-fold symmetric interaction is present in the cyanide hydratases from *G. sorghi* (Woodward et al., 2008) and *N. crassa* (Dent et al., 2008). This interaction, which we have called the 'F' surface, occurs close to the 'D' surface in a region where there is a hole in other homologous enzymes (Figure 4). We have seen helical fibres in which the interactions across the groove are at the D surface only (*B. pumilus* CynD and *R. rhodochrous* J1 nitrilase), both D and F surfaces (*N. crassa* CHT) and the F surface only (*G. sorghi* CHT). The interactions occurring at the 'C', 'D' or 'F' surfaces dictate the helical symmetry (the rotation ($\Delta\phi$) and axial rise ($\Delta z$) of each subunit along the helical axis) and consequently, the number of dimers per turn of the helix.

The enzymes with the 'F' surface interaction are seen to have an increased helical twist (Dent et al., 2008; Woodward et al., 2008). The atomic details of the location of the charged residues in these surfaces are yet to be visualized.

### 7.4 The 'E' surface

The 'E' surface interaction differs from other surfaces because its contributors are asymmetric and arise from different regions of the subunit. Interpretation of the docked three-dimensional map of the *P. stutzeri* AK61 enzyme (Sewell et al., 2003), suggested that spiral elongation occurs via interactions at the 'A' and 'C' surfaces until an opportunity for the 'E' interaction occurs across the groove of the helix. The putative electrostatic interactions which result in helix termination are between residues 266EID268 and 92RKNK95 in the *P. stutzeri* CynD and these may well be unique to this enzyme. The positive residues implicated in this region are located in the carboxy-terminal end of the α3 helix while the negative residues occur at the end of strand β14 (Figure 3). We speculate that the 'E' surface interaction generally involves the conserved negative cluster E/DID and the positive cluster R/K-R/K-X-E/K/X which is not conserved. This interaction distorts the spiral by tilting the terminal dimer such that the diameter is reduced preventing further addition of subunits and causing the cyanide dihydratse spiral to terminate (Sewell et al., 2003). In contrast, the enzyme from *D. melanogaster* does not form a complete spiral due to disorder in the terminal subunits (Lundgren et al., 2008). While the *P. stutzeri* and *G. pallidus* DAC521 enzymes are seen to form short terminating spiral structures, the *R. rhodochrous* J1 nitrilase (Thuku et al., 2007) and the cyanide dihydratase from *B. pumilus* C1 (Jandhyala et al., 2003) occur either as a short or long spirals. Details of the interactions which limit helix formation remain speculative and their proper elucidation is an obvious direction for future research.

## 8. The role of the extended C-terminal region

All the microbial nitrilases for which sequence data are available and the related crystalline amidases are seen to have an extended C-terminal sequence about 40-100 amino acids longer than that of the other homologous structures (Figure 3). The C-terminal region is located on the inside of the spiral. Several amidase structures have allowed visualization of structure in this region but the alpha helical content of the amidases seems to be far greater that of the nitrilases (as predicted by PSIPRED) and the structures may not be transferable (Andrade et al., 2007; Hung et al., 2007; Kimani et al., 2007). Furthermore, the C-terminus in these structures lies on the outside of the hexamer. The *G. pallidus* amidase has 66 amino acids in its carboxy-

terminus. Its tail sequence is folded into four short helices and these interact with the equivalent region arising from the associated subunit to strengthen the interactions at the 'A' surface (Kimani et al., 2007). Earlier roles of the C-terminus involving different structural elements in homologous enzymes with a shorter tail sequence had been suggested in the crystal structures of DCase (Nakai et al., 2000) and the NitFhit protein (Pace et al., 2000). A similar interaction involving a pair of C-terminal helices (one from each subunit), is seen to occur in the enzyme from *Drosophila melanogaster* (Lundgren et al., 2008). However, the tail sequence in this enzyme extends across the surface of the two-fold related monomer where its terminal strand interacts in a parallel manner with another arising from different region of the associated subunit. This interaction anchors the tail of each subunit in the vicinity of the 'C' surface, which implies that this part of the molecule could be necessary for oligomerization and activation. The docking of models of the *N. crassa* enzyme incorporating structural information from the *G. pallidus* amidase places a region of the its C-terminus at the 'C' interface, and raises the possibility that flexibility in the region could position some tail residues from the partner subunit in close proximity to the active site (Dent et al., 2008). This could possibly be the general behavior of the extended C-terminus in the spiral forming enzymes.

Another possible role of the C-terminus is presented in the *B. pumilus* C1 enzyme which lost activity after removal of more than 28 residues (Sewell et al., 2005). We have observed similar results in the nitrilase from *R. rhodochrous* J1 following the truncation of 55 C-terminal residues (Thuku et al., 2007). Clearly, this suggests that a region of the C-terminus is involved at the 'A' and 'C' surfaces and this is important for enzyme oligomerization and activity. A recent study in the tail sequence of the arylacetonitrilase from *Pseudomonas fluorescens* EBC191 concluded that the C-terminal region may be necessary for activity and stability of this enzyme, as well as its enantioselectivity (Kiziak et al., 2007). Modified constructs bearing truncations in the C-terminus of more than 30 amino acids did not show significant changes in enzymatic properties compared to the native enzyme. However, the sequential deletion of between 47-75 amino acids in this region was seen to cause a significant decrease in enzymatic activity and stability. In particular, these structural changes resulted in an increased degree of amide formation and the preference for one enantiomer of mandelonitrile (Kiziak et al., 2007). In contrast, no enantiomeric preference was observed when the substrate was 2-phenylpropionitrile. Furthermore, no significant differences in enzymatic properties were observed when about 50-80 residues in its tail sequence was swapped with those from other

superfamily enzymes, namely *Rhodococcus rhodochrous* NCIMB 11216 (Harper, 1977) and *Alcaligenes faecalis* ATCC 8750 (Yamamoto et al., 1991; 1992). This observation is similar to that reported in the *Bacillus pumilus* CynD which retained activity after its tail sequence was swapped with that from the highly homologous *Pseudomonas stutzeri* enzyme (Sewell et al., 2005). Kiziak and coworkers (2007) also suggested that while the C-terminal region is required for activity and stability, the globular part of the *P. fluorescens* nitrilase could determine the degree of the enantioselectivity that is exerted by the enzyme. This would suggest that during the process the oligomerization, some steric changes could possibly be transmitted altering not only the conformation of the enzyme but also its active site configuration such that only one enantiomer can bind.

A region corresponding to the 'A' surface in the C-terminus of the microbial nitrilases (Figure 3) comprising about 7 residues is predicted by PSIPRED (Bryson et al., 2005) to form a beta strand similar to that seen in the Nit domain of the NitFhit structure (Pace et al., 2000). In the NitFhit structure, this tail region is seen to form an anti-parallel beta sheet across the interface with its equivalent from the partner subunit, and would correspond to the pair of α9 helices in the crystalline amidases (Andrade et al., 2007; Hung et al., 2007, Kimani et al., 2007). The truncation of the C-terminus on either side of this region was seen to disrupt the activity of other homologous enzymes (Sewell et al., 2005; Thuku et al., 2007), and suggests that the C-terminal region is involved in the formation of the 'A' surface in these enzymes as well. Interestingly, several point mutations of a histidine (residue 296) in the sequence of the *P. fluoroscens* EBC191 enzyme with either basic or neutral residues resulted in decreased enzymatic activity and stability, and an increase in amide formation (Kiziak et al., 2007). This histidine appears to be generally conserved in the sequences of the non-crystalline nitrilases and is located in a region (as predicted by PSIPRED) that is close to the part of the tail which interacts across the 'A' surface. This region in the spiral forming nitrilases is preceded by a sequence that conserves the motif 'DP/FXGHY', as previously reported (Kiziak et al., 2007). Our modeling studies show that the imidazole side chain of the histidine residue is positioned facing the 'C' surface and in close proximity to the active site pocket where it could possibly interact with the substrate on its way to the active site.

Additional evidence for the possible role of the C-terminus is seen to occur in the case of the nitrilase from *R. rhodochrous* J1, in which it is necessary to remove residues beyond 327 in its C-terminus in order to form long regular helices (Thuku et al., 2007), otherwise 'c' shaped

aggregates (similar to those of the fruit fly enzyme (Lundgren et al., 2008)) are formed. The natural process leading to the loss of 39 amino acids in the *R. rhodochrous* J1 nitrilase is thought to be an autolysis and helix formation can be reproduced by recombinantly expressing residues 1-327. Interestingly, the expression of either more (1-340) or fewer (1-317) residues, results in the formation of shorter, poorly formed helices. This can be rationalized in terms of the packing in the C-terminal region which is seen to be located in the centre of the helix. The packing in the 1-327 helices is such that the subunits fit optimally and the interacting residues at the 'D' surface align to stabilize the extended assembly. If the packing is too loose as with 1-317 or too tight as with 1-340, only short helices form.

A further interesting effect is seen in the cyanide dihydratase from *B. pumilus* C1. This enzyme changes form from a terminating 18 subunit spiral to a variable length helix as the pH drops from 8 to 5.4 (Jandhyala et al., 2003). This effect is reversible and is accompanied by an increase in the enzyme activity (Jandhyala et al., 2005). The change in quaternary structure strongly implicates the involvement of histidine residues in its C-terminus. This residue has a pKa of 6.05 and the imidazole side chain would acquire a positive charge at this pH. We have studied the enzyme from two different environmental isolates of *B. pumilus*, namely C1 and 8A3 and found that they differ at only 7 positions in their C-terminal sequence (Jandhyala, 2002). The 8A3 isolate does not demonstrate the reversible helix forming phenomenon (Scheffer, 2006). There are 3 histidines in the C-terminal region of the C1 isolate that are absent in the 8A3 isolate. The mechanism suggested for helix formation is one in which the charge repulsion between the C-terminal regions from different subunits and located in the center of the spiral results in an expansion of the radius of the helix, disrupting the 'E' surface interactions, and allowing the spiral to elongate. A slight increase in activity is observed when the helix elongates at pH5.4. It has been suggested that this is due to the terminal monomers in the short spirals being activated by the formation of the 'C' surface once they became part of the extended helices (Jandhyala et al., 2005).

Despite the inherent disorder and lack of conservation in the C-terminal region of the microbial nitrilases, we can conclude that this region has two possible roles: firstly, the tail sequence facilitates spiral formation by positioning residues located at the interfaces in close proximity with each other and thereby strengthening the interfaces and secondly, its inherent flexibility suggests that this region probably interacts with another part of the subunit which is located near the active site in a manner which influences the activity and stability of the spiral.

## 9. Conclusion

Considerable information concerning the structure, mechanism and substrate specificity of the microbial nitrilases is now known or inferred from homologous enzymes. There is considerable potential for transferring this knowledge to industrial applications. The interactions which form the dimer and the spiral are generally conserved within the superfamily enzymes. The 'A' surface interaction (involving α5 and α6 helices) corresponds to the dimer interface and is present in all nitrilase homologues for which the crystal structure has been determined. The 'C' surface interaction occurs between adjacent dimers forming the one-start helix. The docking of homology models in the microbial nitrilases concluded that the density in the 'C' surface is not only filled by residues in the two significant insertions, but also by residues in the C-terminal region. This is the case in the atomic spiral structure of the enzyme from *Drosophila melanogaster* (Lundgren et al., 2008), in which the carboxy-terminus is situated in the center of the spiral and not on the outside as seen in the amidase structures (Andrade et al., 2007; Hung et al., 2007; Kimani et al., 2007). Different interactions are seen to occur across the groove of the helix. The cyanide dihydratases (Sewell et al., 2003; Jandhyala et al., 2003) and the nitrilase from *R. rhodochrous* J1 (Thuku et al., 2007) have a 'D' surface, whereas the cyanide hydratases have either an 'F' surface (Woodward et al., 2008) or both 'D' and 'F' surfaces (Dent et al., 2008). Both the 'D' and the 'F' interactions possibly confer stability to the structure and their occurrence corresponds to the inherent helical twist of the enzyme. The 'E' interaction is asymmetric and causes the spiral to terminate. In the microbial nitrilases, the two-fold, symmetric 'C', 'D' and 'F' surfaces, and the asymmetric 'E' surface have only been visualized in electron microscopic reconstructions and therefore, the details of the interacting residues are yet to be determined at atomic resolution. Even though the details of the spiral termination mechanism are not clear and may not be common, the evidence we have presented suggests that the tendency to form spirals may be widespread in the microbial nitrilases. Several reports have speculated on the biological roles of the nitrilases in prokaryotes and eukaryotes (Banerjee et al., 2002; O'Reilly and Turner, 2003; Robertson et al., 2004). It is not clear what role a helical assembly could play within the cell. However, it has previously been reported that nitrile-hydrolysing activities in filamentous fungi accompany other enzymes involved in the aldoxime-degrading pathway (Kato et al., 2000). In addition, we have previously speculated that a helical assembly could act as a scaffold for other nitrilase-associated proteins leading to an organelle-like assembly of enzymes involved in the same biochemical pathway (Thuku et al., 2007). Clearly, a helical assembly provides a

concentration of active sites, the role of which could possibly be to detoxify harmful nitriles within the organism. This provides an explanation of the previous observation in the fungus *Gloeocercospora sorghi* which expresses high amounts of cyanide hydratase in a high cyanide environment (Wang et al., 1992, 1999). All the spiral structures illustrated in Figure 4 have characteristic holes on their surface and a central channel of unknown function. If we speculate that the helix provides a platform for other associated enzymes to 'dock', then it is possible that the holes and the central cavity act as a channel for substrates and products required by other enzymes, however, there is no evidence of this.

The occurrence of two interacting surfaces across the groove of the helix in the cyanide hydratases (Dent et al., 2008; Woodward et al., 2008), suggests that additional interactions are required to stabilize fragile helices with an increased helical twist. Further stabilizing interactions can be introduced in these surfaces by mutation, for example, by increasing the number of interacting charged residues. This could increase the stability of the helix and potentially lead to enzymes which can be used over a broad pH range and at elevated temperatures. In addition, the long helices could have potential biotechnological applications because they can easily be purified, immobilized, have a high concentration of active sites, and can be stored for long periods. Although the biological roles of nitrilases and their natural substrates are not well understood, their activity with various substrates that have chemical or pharmaceutical importance is widely known. Despite this knowledge, efforts to modify microbial nitrilases using a variety of molecular techniques are still hindered by the unavailability of a crystal structure. Nevertheless, this review provides structural insights gained using different techniques, and which can then be used to inform various on-going research efforts.



**Acknowledgments**

We thank Dr Doreen Dobritzsch for providing us with the protein coordinates for the β-alanine synthase from *Drosophila melanogaster*. We greatly appreciate the substantial support we have received from Carnegie Corporation of New York, the National Research Foundation and the University of Cape Town. RNT was funded by an international scholarship from UCT and a CSIR Biosciences scholarship. Work in the MB lab is funded by the Texas Hazardous Substance Research Center and Robert A. Welch Foundation.

**10. References**

Alamatawah, Q.A., Cramp, R. and Cowan, D.A. (1999). Characterization of an inducible nitrilase from a thermophilic Bacillus. *Extremophiles* **3**, 283-291

Andrade, J., Karmali, A., Carrondo, M.A. and Frazao, C. (2007). Structure of amidase from *Pseudomonas aeruginosa* showing a trapped acyl transfer reaction intermediate state. *J Biol Chem* **282**, 19598-19605

Bandyopadhyay, A.K., Nagasawa, T., Asano, Y., Fujishiro, K., Tani, Y. and Yamada, H. (1986). Purification and characterization of benzonitrilases from *Arthrobacter* sp. Strain J-1. *Appl Environ Microbiol* **51**, 302-306

Banerjee, A., Sharma, R. and Banerjee, U.C. (2002). The nitrile-degrading enzymes: current status and future prospects. *Appl Microbiol Biotechnol* **60**, 30-44

Banerjee, A., Kaul, P. and Banerjee, U.C. (2006). Purification and characterization of an enantioselective arylacetonitrilase from *Pseudomonas putida*. *Arch Microbiol* **184**, 407-418

Barclay, M., Tett, V.A. and Knowles, C.J. (1998). Metabolism and enzymology of cyanide/metallocyanide biodegradation by *Fusarium solani* under neutral and acidic conditions. *Enzyme Microb Technol* **23**, 321-330

Bartel, B. and Fink, G.R. (1994). Differential regulation of an auxin-producing nitrilase gene family in *Arabidopsis thaliana*. *Proc Nat Acad Sci* USA **91**, 6649-6653

Bartling, D., Seedorf, M., Mithofer, A. and Weiler, E.W. (1992). Cloning and expression of an *Arabidopsis* nitrilase which can convert Indole-3-acetonitrile to the plant hormone, Indole-3-acetic acid. *Eur J Biochem* **205**, 417-424

Bartling, D., Seedorf, M., Schimdt, R.C. and Weiler, E.W. (1994). Molecular characterization of two cloned nitrilases from *Arabidopsis thaliana*: key enzymes in biosynthesis of plant hormone indole -3- acetic acid. *Proc Nat Acad Sci* USA **91**, 6021-5

Baxter, J. and Cummings, S.P. (2006). The current and future applications of microorganisms in the bioremediation of cyanide contamination. *Antonie Leeuwenhoek* **90**, 1–17

Bhalla, T.C., Miura, A., Wakamoto, A., Ohba, Y. and Furuhasi, K. (1992). Asymmteric hydrolysis of α-aminonitriles to optically active aminoacids by a nitrilase of *Rhodococcus rhodochrous* PA-34. *Appl Microbiol Biotechnol* **37**, 184-190

Bellinzoni, M., Buroni, S., Pasca, M.R., Guglierame, P., Arcesi, F., De Rossi, E. and Riccardi, G. (2005). Glutamine amidotransferance activity of NAD+ synthetase from *Mycobacterium tuberculosis* depends on an amino-terminal nitrilase domain. *Res Microbiol* **156**, 173-177

Brady, D., Beeton, A., Zeevaart, J., Kgaje, C., van Rantwijk, F. and Sheldon, R.A. (2004). Characterisation of nitrilase and nitrile hydratase biocatalytic systems. *Appl Microbiol Biotechnol* **64**, 76-85

Brady, D., Dube, N. and Pettersen, R. (2006). Green Chemistry: Highly selective biocatalytic hydrolysis of nitrile compounds. *S Afr J Sci* **102**, 339-344

Brenner, C. (2002). Catalysis in the nitrilase superfamily. *Curr Opin Struct Biol* **12**, 775-782.

Chauhan, S., Wu, S., Blumerman, W.S., Fallon, R.D., Gavagan, J.E., DiCosimo, R. and Payne, M.S. (2003). Purification, cloning, sequencing and over-expression in *Escherichia coli* of a regioselective aliphatic nitrilase from *Acidovorax facilis* 72W. *Appl Microbiol Biotechnol* **61**, 118-122

Chin, K-H., Tsai, Y-D., Chan, N-L., Huang, K-F., Wang, A. H-J. and Chou, S-H. (2007). The crystal structure of XC1258 from *Xanthomonas campestris*: A putative prokaryotic Nit protein with an arsenic adduct in the active site. *Proteins: Struct Funct Bioinform* **69**, 665-671

Chen, C., Chiu, W., Liu, J., Hsu, W. and Wang, W-C. (2003). Structural basis for catalysis and substrate specificity of *Agrobacterium radiobacter* N-Carbamoyl-D-amino acid amidohydrolase. *J Biol Chem* **278**, 26194–26201

Cluness, M.J., Turner, P.D., Clements, E., Brown, D.T. and O'Reilly, C. (1993). Purification and properties of cyanide hydratase from *Fusarium lateritium* and analysis of the corresponding chy1 gene. *J Gen Microbiol* **139**, 1807-1815

Cohen, G.H. (1997). ALIGN: a program to superimpose protein coordinates, accounting for insertions and deletions. *J Appl Crystallogr* **30**, 1160-1161

DeLano, W.L. (2002). The PyMOL Molecular Graphics System. DeLano Scientific, Palo Alto, CA, USA. http://www.pymol.org

Dent, K.C., Weber, B.W., Benedik, M.J. and Sewell, B.T. (2008). The helical structure of the cyanide dihydratase from *Neurospora crassa*. *Appl Microbiol Biotechnol* (*submitted*)

DeSantis, G., Zhu, Z., Greenberg, W.A., Wong, K., Chaplin, J., Hanson, S.R., Farewell, B., Nicholson, L.W., Rand, C.L., Weiner, D.P., Robertson, D.E. and Burk, M.J. (2002). An enzyme library approach to biocatalysis: Development of nitrilases for enantioselective production of carboxylic acid derivatives. *J Am Chem Soc* **124**, 9024-9025

DeSantis, G., Wong, K., Farewell, B., Chatman, K., Zhu, Z., Tomlinson, G., Huang, H., Tan, X., Bibbs, L., Chen, P., Kretz, K. and Burk, M.J. (2003). Creation of a productive, highly enantioselective nitrilase through Gene Site Saturation Mutagenesis (GSSM). *J Am Chem Soc* **124**, 11476-11477

Dhillon, J.K. and Shivaraman, N. (1999a). Biodegradation of cyanide compounds by a *Pseudomonas* species S1. *Can J Microbiol* **45**, 201-208.

Dhillon, J.K., Chatre, S., Shanker, R. and Shivaraman, N. (1999b). Transformation of aliphatic and aromatic nitriles by a nitrilase from *Pseudomonas* sp. *Can J Microbiol* **45**, 811-815.

Dohmoto, M., Sano, J., Tsunoda, H. and Yamaguchi, K. (1999). Structural analysis of TNIT4 genes encoding nitrilase-like protein from Tobacco. *DNA Res* **6**, 313-317

Dohmoto, M., Tsunoda, H., Isaji, G., Chiba, R. and Yamaguchi, K. (2000). Genes encoding nitrilase-like protein from Tobacco. *DNA Res* **7**, 283-289

Effenberger, E. and Osswald, S. (2001). Selective hydrolysis of aliphatic dinitriles to monocarboxylic acids by a nitrilase from *Arabidopsis thaliana*. *Synthesis* **12**, 1866-1872

Fernandes, B.C.M., Mateo, C., Kiziak C., Chmura, A., Wacker, J., van Rantwijk, F., Stolz, A., and Sheldon R.A. (2006). Nitrile hydratase activity of a recombinant nitrilase. *Adv Synth Catal* **348**, 2597-2603

Fry, W.E. and Munch, D.C. (1975). Hydrogen cyanide detoxification by *Gloeocercospora sorghi*. *Physiol Plant Pathol* **7**, 23-33

Gagavan, J.E., DiCosimo, R., Eisenberg, A., Fager, S.K., Folsom, P.W., Hahn, E.C., Schneider, K.J. and Fallon, R.D. (1999). A gram-negative bacterium producing a heat-stable nitrilase highly active on aliphatic dinitriles. *Appl Microbiol Biotechnol* **52**, 654-659

Gradley, M.L. and Knowles, C.J. (1994). Asymmetric hydrolysis of chiral nitriles by *Rhodococcus rhodochrous* NCIMB 11216 nitrilase. *Biotechnol Lett* **16**, 41-46

Goldlust, A. and Bohak, Z. (1989). Induction, purification, and characterization of the nitrilase of *Fusarium oxysporum* f.sp *melonis*. *Biotechnol Appl Biochem* **11**, 581-601

Harper, D.B. (1977a). Fungal degradation of aromatic nitriles: enzymology of C-N cleavage by *Fusarium solani*. *Biochem J* **167**, 685-692

Harper, D.B. (1977b). Microbial metabolism of aromatic nitriles: enzymology of C-N cleavage by *Norcadia* sp. (*Rhodochrous* group) NCIB 11216. *Biochem J* **165**, 309-319

Harper, D.B. (1985). Characterization of a nitrilase from *Norcadia* sp. (*Rhodochrous* group) NCIB 11215, using *p*-hydroxybenzonitrile as sole carbon source. *Int J Biochem* **17**, 677-683

Hashimoto, H., Aoki, M., Shimizu, T., Nakai, T., Morikawa, H., Ikenaka, Y., Takahashi, S. and Sato, M. (2004). Crystal Structure of C171A/V236A Mutant of N-carbamyl-D-amino acid amidohydrolase. RCSB Protein Data Bank (1uf5)

Heinemann, U., Engels, D., Burger, S., Kiziak, C., Mattes, R. and Stolz, A. (2003). Cloning of a nitrilase gene from the cyanobacterium *Synechocystis* sp. Strain PCC6803 and heterologous expression and characterization of the encoded protein. *Appl Environ Microbiol* **69**, 4359-4366

Hook, R.H. and Robinson, W.G. (1964). Ricinine nitrilase II: Purification properties. *J Biol Chem* **239**, 4263-4267

Hoyle, A.J., Bunch, A.W. and Knowles, C.J. (1998). The nitrilases of *Rhodococcus rhodochrous* NCIMB 11216. *Enzyme Microb Technol* **23**, 475-482

Hung, C.L., Liu, J.H., Chiu, W.C., Huang, S.W. and Wang, W-C. (2007). Crystal structure of *Helicobacter pylori* Formamidase AmiF reveals a cysteine-glutamate-lysine catalytic triad. The *J Biol Chem*, **282**, 12220-12229

Ingvorsen, K., H∅jer-Pedersen, B. and Godtfredsen, S.E. (1991). Novel cyanide hydrolysiing enzyme from *Alcaligenes xylosoxidans* subsp. *denitrificans*. *Appl Environ Microbiol* **57**, 1783-1789

Jandhyala, D.M., (2002) Cyanide degrading nitrilases for detoxification of cyanide containing waste waters. PhD thesis, University of Houston

Jandhyala, D.M., Berman, M., Meyers, P.R., Sewell, B.T., Willson, R.C. and Benedik, M.J. (2003). Cyn D, the cyanide dihydratase from *Bacillus pumillus*: Gene cloning and structural studies. *Appl Environ Microbiol* **69**, 4794-4805

Jandhyala, D.M., Willson, R.C., Sewell, B.T. and Benedik, M.J. (2005). Comparison of cyanide degrading nitrilases. *Appl Microbiol Biotechnol* **68**, 327-335

Jenrich, R., Trompetter, I., Bak, S., Olsen, C.E., Moller, B.L. and Piotrowski, M. (2007). Evolution of heteromeric nitrilase complexes in *Poaceae* with new functions in nitrile metabolism. *Proc Nat Acad Sci* USA **104**, 18848-18853

Jones, D.T. (1999). GenTHREADER: An efficient and reliable protein fold recognition method for genomic sequences. *J Mol Biol* **287**, 797-815

Karmali, A., Pacheco, R., Tata, R. and Brown., P. (2001). Substitutions of thr-103-ile and trp-138-gly in amidase from *Pseudomonas aeruginosa* are responsible for altered kinetic properties and enzyme instability. *Mol Biotech* **17**, 201-212

Kaplan, O., Vejvoda, V., Pisvejcova, C.A. and Martinkova, L. (2006a). Hyperinduction of nitrilases in filamentous fungi. *J Ind Microbiol Biotechnol* **33**, 891-896

Kaplan, O., Nikolau, K., Pisvejcova, C.A. and Martinkova, L. (2006b). Hydrolysis of nitriles and amides by filamentous fungi. *Enzyme Microb Technol* **38**, 260-264

Kaplan, O., Vejvoda, V., Plihal, O., Pompach, P., Kavan, D., Bojarova, P., Bezouska, K., Mackova, M., Cantarella, M., Jirku, V., Kren, V. and Martinkova, L. (2006c). Purification and characterization of a nitrilase from *Aspergillus niger* K10. *Appl Microbiol Biotechnol* **73**, 567-575

Kato, Y., Nakamura, K., Sakiyama, H., Mayhew, S.G. and Asano, Y. (2000). Novel Heme-containing lyase, phenylacetaldoxime dehydratase from *Bacillus sp*. strain OxB-1: Purification, Characterization, and Molecular cloning of the gene. *Biochem* **39**, 800-809

Kimani, S.W., Agarkar, V.B., Cowan, D.A., Sayed, M.F-R. and Sewell, B.T. (2007). Structure of an aliphatic amidase from *Geobacillus pallidus* RAPc8. *Acta Crystallogr* Sect D: *Biol Crystallogr* **63**, 1048-1048

Kiziak, C., Conradt, D., Stolz, A., Mattes, R. and Klein, J. (2005). Nitrilase from *Pseudomonas fluorescens* EBC191: cloning and heterologous expression of the gene and biochemical characterization of the recombinant enzyme. *Microbiology* **151**, 3639-3648

Kiziak, C., Klein, J. and Stoltz, A. (2007). Influence of different carboxy-terminal mutations on the substrate-, reaction- and enantiospecificity of the arylacetonitrilase from *Pseudomonas fluorescens* EBC191.*Prot Eng Des Sel* **20**, 385-396

Kobayashi, M., Nagasawa, T. and Yamada, H. (1988). Regiospecific hydrolysis of dinitrile compounds by nitrilase from *Rhodococcus rhodochrous* J1. *Appl Microbiol Biotechnol* **29**, 231-233

Kobayashi, M., Nagasawa, T. and Yamada, H. (1989). Nitrilase of *Rhodococcus rhodochrous* J1: Purification and characterization. *Eur J Biochem* **182**, 349-356

Kobayashi, M., Yanaka, N., Nagasawa, T. and Yamada, H. (1990). Purification and characterization of a novel nitrilase of *Rhodococcus rhodochrous* K22 that acts on aliphatic nitriles. *J Bacteriol* **172**, 4807-4815

Kobayashi, M., Yanaka, N., Nagasawa, T. and Yamada, H. (1992). Primary structure of an aliphatic nitrile-degrading enzyme, aliphatic nitrilase, from *Rhodococcus rhodochrous* K22 and expression of its gene and identification of the active site residue. *Biochem* **31**, 9000-9007

Kobayashi, M. and Shimizu, Y. (1994). Versatile nitrilases: nitrile-hydrolyzing enzymes. *FEMS Microbiol Lett* **120**, 217-224

Kriechbaumer, V., Park, W.J., Piotrowski, M., Meeley, R.B., Gierl, A. and Glawischnig, E. (2007). Maize nitrilases have a dual role in auxin homeostasis and β-cyanoalanine hydrolysis. *J Exp Bot* **58**, 4225-4233

Kumaran, D., Eswaramoorthy, S., Gerchman, S.E., Kycia, H., Studier, F.W. and Swaminathan, S. (2003). Crystal structure of putative CN hydrolase from yeast. *PROTEINS: Struct Funct Genet* **52**, 283–291

Kunz, D.A., Wang, C.S. and Chen, J.L. (1994). Alternative routes of enzymatic cyanide metabolism in *Pseudomonas fluorescens* NCIMB 11764. *Microbiology* **140**, 1705-1712

Layh, N., Paratt, J. and Willets, A. (1998). Characterization and partial purification of an enantioselective arylacetonitrilase from *Pseudomonas fluorescens* DSM7155. *J Mol Catal B: Enzym* **5**, 467-474

Levy-Schil, S., Soubrier, F., Crutz-le Coq, A.M., Faucher, D., Crouzet, J. and Petre, D. (1995). Aliphatic nitrilase from a soil-isolated *Comamonas testoteroni* sp: gene cloning and over expression, purification and primary structure. *Gene* **161**, 15-20

Lundgren, S., Lohkamp, B., Andersen, B., Piskur, J. and Dobritzsch, D. (2008). The crystal structure of B-alanine synthase from *Drosophila melanogaster* reveals a homoactameric helical turn-like assembly. *J Mol Biol* **377**, 1544-1559

Martinkova L, Vejvoda V and and Kren V (2008). Selection and screening for enzymes of nitrile metabolism. *J Biotechnol*, **133**, 318-326

Mathew, C.D., Nagasawa, T., Kobayashi, M. and Yamada, H. (1998). Nitrilase catalyzed production of nicotinic acid from 3-cyanopyridine in *Rhodococcus rhodochrous* J1. *Appl Environ Microbiol* **54**, 1030-1032

McBride, K.E., Kenny, J.W. and Stalker, D.M. (1986). Metabolism of the herbicide bromoxynil by *Klebsiella pneumonia* subsp. *ozaenae*. *Appl Environ Microbiol* **52**, 325-330

McGuffin, L.J., Bryson, K. and Jones, D.T. (2000). The PSIPRED protein structure prediction server. *Bioinformatics* **16**, 404-405

McGuffin, L.J. and Jones, D.T. (2003). Improvement of the GenTHREADER method for genomic fold recognition. *Bioinformatics* **19**, 874-881

Meyers, P.R., Rawlings, D.E., Woods, D.R., and Lindsey, G.G. (1993). Isolation and characterization of a cyanide dihydratase from *Bacillus pumilus* C1. *J Bacteriol* **175**, 6105-6112

Mizuguchi, K., Deane, C.M., Blundell, T.L., Johnson, M.S. and Overington, J.P. (1998). JOY: protein sequence-structure alignments representation and analysis. *Bioinformatics* **14**, 617-623

Mueller, P., Egarova, K., Vorgias, E.C., Boutou, E., Trauthwein, H., Verseck, S. and Antranikian, G. (2006). Cloning, expression and characterization of a thermoactive nitrilase from the hyperthermophile archaeon *Pyrococcus abyssi*. *Protein Expression Purif* **47**, 672-681

Nagasawa, T., Mauger, J. and Yamada, H. (1990). A novel nitrilase, arylacetonitrilase, of *Alcaligenes faecalis* JM3: Purification and characterization. *Eur J Biochem* **194**, 765-772

Nagasawa, T., Wieser, M., Nakamura, T., Iwahara, H., Yoshida, T. and Gekko, K. (2000). Nitrilase of *Rhodococcus rhodochrous* J1: Conversion into the active form by subunit association. *Eur J Biochem* **267**, 138-144

Nakai, T., Hasegawa, T., Yamashita, E., Yamamoto, M., Kumasaka, T., Ueki, T., Nanba, H., Ikenaka, Y., Takahashi, S., Sato, M. and Tsukihara, T. (2000). Crystal structure of *N*-carbamyl-D-amino acid amidohydrolase with a novel catalytic framework common to amidohydrolases. *Structure* **8**, 729–739

Nolan, L.M., Harnedy, P.A., Turner, P., Hearne, A.B. and O'Reilly, C. (2003). The cyanide hydratase enzyme of *Fusarium lateritium* also has nitrilase activity. *FEMS Microbiol Lett* **221**, 161-165

O'Reilly, C. and Turner, P.D. (2003). The nitrilase family of CN hydrolyzing enzymes – a comparative study. *J Appl Microbiol* **95**, 1161-1174

Osswald, S., Wajant, H. and Effenberger, F. (2002). Characterization and synthetic applications of recombinant AtNIT1 from *Arabidopsis thaliana*. *Eur J Biochem* **269**, 680-687

Pace, H.C., Hodawadekar, S.C., Draganescu, A., Huang, J., Bieganowski, P., Pekarsky, Y., Croce, C.M. and Brenner, C. (2000). Crystal structure of the worm NitFhit Rosetta Stone protein reveals a Nit tetramer binding two Fhit dimers. *Curr Biol* **10**, 907–917

Pace, H. and Brenner, C. (2001). The nitrilase superfamily: classification, structure and function. *Genome Biol* **2**, 1-9

Panova, A., Mersinger, L.J., Liu, Q., Foo, T., Roe, D.C., Spillan, W.L., Sigmund, A.E., Ben-Bassat, A., Wagner, L.W., O'Keefe, D.P., Wu, S., Petrillo, K.L., Payne, M.S., Breske, S.T, Gallagher, F.G., Dicosimo, R. (2007). Chemoenzymatic synthesis of glycolic acid. *Adv Synth Catal* **349**, 1462-1474

Park, W.J., Kriechbaumer, V., Muller, A., Piotrowski, M., Meeley, R.B., Gierl, A. and Glawischnig, E. (2003). The nitrilase ZmNIT2 converts indole-3-acetonitrile to indole-3-acetic acid. *Plant Physiol* **133**, 794-802

Pettersen, E.F., Goddard, T.D., Huang, C.C., Couch, G.S., Greenblatt, D.M., Meng, E.C. and Ferrin, T.E. (2004). UCSF Chimera - A visualization system for exploratory research and analysis. *J Comput Chem* **25**, 1605-1612

Piotrowski, M., Schonfelder, S. and Weiler, E.R. (2001). The *Arabidospsis thaliana* isogene NIT4 and its orthologs in Tobacco encode β-cyano-L-alanine hydratase/nitrilase. *J. Biol Chem* **276**, 2616-2621

Podar, M., Eads, J.R. and Richardson, T.H. (2005). Evolution of a microbial nitrilase gene family: a comparative and environmental genomics study. *BMC Evol Biol* **5**, 1-13

Robertson, D.E., Chaplin, J.A., DeSantis, G., Podar, M., Madden, M., Chi, E., Richardson, T., Milan, A., Miller, M., Weiner, D.P., Wong, K., McQuaid, J., Farwell, B., Preston, L.A., Tan, X., Snead, M.A., Keller, M., Mathur, E., Kretz, P.L., Burk, M.J. and Short, J.M. (2004). Exploring nitrilase sequence space for enantioselective catalysis. *Appl Environ Microbiol* **70**, 2429-2436

Robinson, W.G. and Hook, R.H. (1964) Ricinine nitrilase I: Reaction product and substrate specificity. *J Biol Chem* **239**, 4257–4262

Sakai, N., Tajika, Y., Yao, M., Watanabe, N. and Tanaka, I. (2004). Crystal structure of hypothetical protein PH0642 from *Pyrococcus horikoshii* at 1.6 Å resolution. *Proteins: Struct Funct Bioinform* **57**, 869–873

Scheffer, M.P. (2006). Helical structures of the cyanide degrading enzymes from *Gloeocercospora sorghi* and *Bacillus pumilus* providing insights into nitrilase quaternary interactions. M.Sc Thesis, University of Cape Town

Schnackerz, K.D. and Dobritzsch, D. (2008). Amidohydrolases of the reductive pyrimidine catabolic pathway Purification, characterization, structure, reaction mechanisms and enzyme deficiency. *Biochim Biophys Acta* **1784**, 431-444

Sewell, B.T., Berman, M.N., Meyers, P.R., Jandhyala, D. and Benedik, M.J. (2003). The cyanide degrading nitrilase from *Pseudomonas stutzeri* AK61 is a two-fold symmetric, 14-subunit spiral. *Structure* **11**, 1-20

Sewell, B.T, Thuku, R.N., Zhang, X. and Benedik, M.J. (2005). The oligomeric structure of nitrilases: the effect of mutating interfacial residues on activity. *Ann NY Acad Sci* **1056**, 153-159

Singh, R., Sharma, R., Tewari, N., Geetanjali, and Rawat, D.S. (2006). Nitrilase and its application as a 'green' catalyst. *Chem Biodivers* **3**, 1279-1287

Snajdrova, R., Myelerova-Kristova, V., Crestia, D., Nikolaou, K., Kuzma, M., Lemaire, M., Galienne, E., Bolte, J., Bezouska, K., Kren, V. and Martinkova, L. (2004). Nitrile biotransformation by *Aspergillus niger*. *J Mol Catal B: Enzym* **29**, 227-232

Stalker, D.M., Malyj, L.D. and McBride, K.E. (1988a). Purification and properties of a nitrilase specific for the herbicide bromoxynil and corresponding nucleotide sequence analysis of the *bxn* gene. *J Biol Chem* **263**, 6310-6314

Stalker, D.M., McBride, K.E. and Malyj, L.D. (1988b). Herbicide resistance in transgenic plants expressing a bacterial detoxification gene. *Science* **242**, 419-423

Stalker, D.M., Kiser, J.A., Baldwin, G., Coulombe, B. and Houck, C.M. (1996). Cotton weed control using the BXN system. In *Herbicide Resistant Crops* ed. O Duke, S. pp 93-105. Boca Raton (Florida), CRC press (Lewis Publishers)

Stevenson, D.E., Feng, R., Dumas, F., Groleau, D., Mihoc, A. and Storer, A.C. (1992). Mechanistic and structural studies on *Rhodococcus* ATCC 39484 nitrilase. *Biotechnol Appl Biochem* **15**, 283-302

Thuku, R.N., Weber, B.W., Varsani, A. and Sewell, B.T. (2007). Post-translational cleavage of recombinantly expressed nitrilase from *Rhodococcus rhodochrous* J1 yields a stable, active helical form. *FEBS J* **274**, 2099–2018

Vejvoda, V., Kaplan, O., Klozova, J., Masak, J., Cejkova, A., Jirku, V., Stloukal, R. and Martinkova, L. (2006a). Mild hydrolysis of nitriles by *Fusarium solani* strain O1. *Folia Microbiol* **51**, 251-256

Vejvoda, V., Kaplan, O., Bezouska, K. and Martinkova, L. (2006b). Mild hydrolysis of nitriles by the immobilized nitrilase from *Aspergillus niger* K10. *J Mol Catal B: Enzym* **39**, 55-58

Vejvoda, V., Kaplan, O., Kubac, D., Kren, V. and Martinkova, L. (2006c). Immobilization of fungal nitrilase and bacterial amidase – two enzymes working in accord. *Biocatal Biotransform* **24**, 414-418

Vejvoda, V., Kaplan, O., Bezouska, K., Pompach, P., Sulc, M., Cantarella, M., Benada, O., Uhnakova, B., Rinagelova, A., Lutz-Wahl, S., Fischer, L., Kren, V. and Martinkova, L. (2008). Purification and characterization of a nitrilase from *Fusarium solani* O1. *J Mol Catal B: Enzym* **50**, 99-106

Wang, P., Mathews, D.E. and VanEtten, H.D. (1992a). Cloning and properties of a cyanide hydratase gene from the phytopathogenic fungus *Gloeocercospora sorghi*. *Biochem Biophys Res Commun* **187**, 1048-1054

Wang, P., Mathews, D.E. and VanEtten, H.D. (1992b). Purification and characterization of cyanide hydratase from the phytopathogenic fungus *Gloeocercospora sorghi*. *Arch Biochem Biophys* **298**, 569-575

Wang, W-C., Hsu, W.H., Chien, F.T. and Chen, C-Y. (2001). Crystal structure and site-directed mutagenesis studies of N-Carbamoyl-D-amino-acid amidohydrolase from *Agrobacterium radiobacter* reveals a homotetramer and insight into a catalytic cleft. *J Mol Biol* **306**, 251-261

Watanabe, A., Yano, K., Ikebukuro, K. and Karube, I. (1998). Cyanide hydrolysis in a cyanide-degrading bacterium, *Pseudomonas stutzeri* AK61, by cyanidase. *Microbiol* **144**, 1677-1682

Woodward, J.D., Weber, B.W., Scheffer, M.P., Benedik, M.J., Hoenger, A. and Sewell, B.T. (2008). Helical structure of unidirectionally shadowed metal replicas of cyanide hydratase from *Gloeocercospora sorghi*. *J Struct Biol* **161**, 111-119

Wu, S., Fogiel, A.J., Petrillo, K.L., Hann, E.C., Mersinger, L.J., DiCosimo, R., O'Keefe, D.P., Ben-Bassat, A. and Payne, M.S. (2007). Protein engineering of *Acidovorax facilis* 72W nitrilase for bioprocess development. *Biotechnol Bioeng* **97**, 698-693

Wu, S., Fogiel, A.J., Petrillo, K.L., Jackson, R.E, Parker, K.N., DiCosimo, R., Ben-Bassat, A., O'Keefe, D.P. and Payne, M.S. (2008). Protein engineering of nitrilase for chemoenzymatic production of glycolic acid. *Biotechnol Bioeng* **99**, 717-720

Yamamoto, K., Oishi, K., Kawakami, K. and Komatsu, K. (1991). Production of R-(-)-Mandelic acid from a Mandelonitrile by *Alcaligenes faecalis* ATCC 8750. *Appl Environ Microbiol* **57**, 3028-3032

Yamamoto, K., Fijimatsu, I. and Komatsu, K. (1992). Purification and characterization of the nitrilase from *Alcaligenes faecalis* ATCC 8750 responsible for enantioselective hydrolysis of mandelonitrile. *J Ferment Bioeng* **73**, 425-430

Yanase, H., Sakamoto, A., Okamoto, K., Kita, K. and Sato, Y. (2000). Degradation of the metal-cyano complex tetracyanonickelate (II) by *Fusarium oxysporum* N-10. *Appl Microbiol Biotechnol* **53**, 328-334

Zheng, Y-G., Chen, J., Liu, Z-Q., Wu, M-H., Xing, L-Y. and Shen, Y-C. (2007). Isolation, identification and characterization of *Bacillus subtilis* ZJB-063, a versatile nitrile-converting bacterium. *Appl Microbiol Biotechnol* **77**, 985-993

Zhu, D., Murkherjee, C., Biehl, E.R. and Hua, L. (2007). Discovery of a mandelonitrile hydrolase from *Bradyrhizobium japonicum* USDA110 by rational genome mining. *J Biotechnol* **129**, 645-650

Zhu, D., Murkherjee, C., Yang, Y., Rios, B.E., Gallagher, D.T., Smith, N.N., Biehl, E.R. and Hua, L. (2008). A new nitrilase from *Bradyrhizopium japonicum* USDA 110: Gene cloning, biochemical characterization and substrate specificity. *J Biotechnol* **133**, 327-333

## Figure Legends

**Figure 1 a**. Stereo view of a dimer model of the nitrilase from *Rhodococccus rhodochrous* J1. The model was built based on structural homology to the nitrilase-related atomic structures of 1erz, 1j31, 1ems and 2vhi (Nakai et al., 2000; Sakai et al., 2004, Pace et al., 2000 and Lundgren et al., 2008, respectively). The association surfaces are indicated in black. The conserved catalytic residues are shown as spheres. The alpha helices (α1, α3, α5 and α6) involved in the interacting surfaces are also highlighted. The figure was produced using PyMOL (DeLano, 2002)**. b**. A close-up view of the 'C' surface loop and the 'catalytic tetrad' in the active site of the model of the nitrilase from *R.rhodochrous* J1. The active site comprises a cysteine (C165), a lysine (K131), and two glutamates (E48 and E138). The location of E138 in a 'C' surface loop raises the possibility that association of dimers moves this residue (which

corresponds to E142 in the amidase structure from *Geobacillus pallidus* (Kimani et al., 2007)) into the correct position for catalytic activity. The figure was produced using PyMOL (DeLano, 2002).

**Figure 2**. The crystal structure of the nitrilase-related β-alanine synthase from *Drosophila melanogaster* (Lundgren et al., 2008). The association of the dimers occurs across the 'C' surface (black arrow) leading to a left-handed octameric assembly which does not close or complete a turn of the helix. The shape of the octamer appears similar to the 'c' shaped oligomers of the nitrilase from *Rhodococcus rhodochrous* J1 (Thuku et al., 2007). The fruit fly enzyme has an extended N-terminus (comprising 60-70 amino acids) which forms a four helical bundle (two from each subunit, grey) across the dimer interface. The C-terminus is located in the center of the spiral assembly. The figure was produced using PyMOL (DeLano, 2002).

**Figure 3.** Multiple alignment of the sequences of the microbial nitrilases studied by us with those of the eleven members in the nitrilase superfamily for which structural information is available, namely 1j31, 1f89, 1ems, 1erz, 1fo6, 1uf5, 2e11, 2dyu, 2uxy and 2plq and 2vhi (Sakai et al., 2004; Kumaran et al., 2003; Pace et al., 2000; Nakai et al., 2000; Wang et al., 2001 Hashimoto et al.,2004; Chin et al., 2007; Hung et al., 2007; Andrade et al., 2007, Kimani et al., 2007 and Lundgren et al., 2008, respectively). The first seven sequences represent nitrilases from *Geobacillus pallidus* DAC521 (Dac521, accession no ABH04285) and *Rhodococcus rhodochrous* J1 (RrJ1, Accession no BAA01994), the cyanide dihydratases from *Bacillus pumilus* strain C1 (BpumC1, accession no AAN77004) and strain 8A3 (Bpum8A3, accession no AAN77003), *Pseudomonas stutzeri* AK61 (PstuCDH, accession no BAA11653), and the cyanide hydratases from *Gloecercospora sorghi* (GsorCH, P32964) and *Neurospora crassa* (NcraCH, accession no XP_960160). Two significant insertions in their sequences relative to the solved structures are located at the 'C' surface. In addition, the microbial nitrilases and the crystalline amidases (2dyu, 2plq and 2uxy) have an extended C-terminus than the other atomic homologues. The prediction of secondary structure using PSIPRED (Bryson et al., 2005) in the C-terminal region is different in all the superfamily enzymes and none of the homologues suggests a suitable model in this region. The β-alanine synthase from the *D. melanogaster* (PDB code 2vhi) has an extended N-terminus (about 60 amino acids) comprising four alpha helices of which a pair (one from each monomer) interact to strengthen the 'A' surface (Lundgren et al., 2008). The conserved active site residues are shown in a box

outline. The position of the glutamate residue (E142 in *G. pallidus* amidase, PDB code 2plq), which has been implicated in the nitrilase reaction mechanism (Kimani et al., 2007) is conserved in all the superfamily enzymes (bold, double underline). The approximate regions of the interacting surfaces, namely 'A', 'C', 'D' and 'E' are indicated on the top line. Charged residues which are possibly involved in the interactions at the 'C', 'D' and 'E' surfaces are highlighted in red (negatively charged) and blue (positively charged). The external loop regions are shaded grey. In the crystal structures of 1erz, 1f89, 1uf5, 2dyu, 2e11, 2uxy, 2plq and 2vhi, the residues reported lining the active site pocket are highlighted in cyan. The differing residue positions in the C-terminal region between the *B. pumilus* strains are highlighted in yellow. The conserved sequence motif 'DP/FXGHY' in the tail region of the spiral forming nitrilases is underlined, and in which a conserved histidine (corresponding to H296 in the enzyme from *Pseudomonas fluorescens* EBC 191 (Kiziak et al., 2005)), is coloured green. The residues missing in the crystal structures are white on a black background. The alignment was constructed by hand based on the predictions by the program mGenTHREADER (Jones, 1999; McGuffin and Jones, 2003); while structural alignment was done using ALIGN (Cohen, 1997). The sequences of the nitrilase homologues with known structures are highlighted in JOY notation (Miziguchi et al., 1998). The secondary structural elements identified in 2plq (Kimani et al., 2007) are indicated in the bottom line. The symbol # in the top line indicates the position in the homologues at which the mutations indicated in Table 2 occur. * indicates the locations of the four active site residues and four glycines that are conserved in all homologues. A multiple sequence alignment of the characterized plant and microbial nitrilases against those of eleven members in the nitrilase superfamily for which structural information is available, is provided as supplementary information.

**Figure 4**. Three dimensional electron microscopic reconstructions of the microbial nitrilases studied by us at low-resolution. These include (from left to right), the terminating 14- subunit spiral of the cyanide dihydratase from *Pseudomonas stutzeri* AK61 (Sewell et al., 2003), the variable length helices of the cyanide dihydratase from *Bacillus pumilus* C1 at pH 5.4 ($\Delta\phi$ = -77$^{o}$, $\Delta z$ = 15 Å, Scheffer, 2006) and the C-terminal truncated nitrilase from *Rhodococcus rhodochrous* J1 ($\Delta\phi$ = -73.5, $\Delta z$ = 15.8 Å, Thuku et al., 2007), and the cyanide hydratases from *Neurospora crassa* (($\Delta\phi$ = -66.7$^{o}$, $\Delta z$ = 13.6 Å, Dent et al., 2008) and *Gloecercospora sorghi* (($\Delta\phi$ = 66$^{o}$, $\Delta z$ = 13 Å, Woodward et al., 2008), respectively. The shape of the dimer and the connectivity defining a left-handed one-start spiral can clearly be discerned. The 'A' surface is

preserved in all members of the nitrilase superfamily. All structures conserve a two-fold axes at the dimer interface ( the 'A' surface) whose line passes through a hole on the other side of the spiral in the case of the nitrilase and cyanide dihydratases, or through the 'F' surface in the case of the fungal cyanide hydratases. A second dyad is found to occur at the 'C' surface with a line passing through the 'D' surface on the other side of the spiral. The 'E' surface is asymmetric and is found to occur specifically in the terminating spiral. The conservation of the insertions at the 'C' surface and the possibility of salt bridge formation across the groove of the helix (at either the 'D' or 'F' surface) suggest that spiral formation may be common among the microbial nitrilases. The figure was produced using UCSF Chimera (Pettersen et al., 2004).

**Figure 5**. The docking of *Rhodococcus rhodochrous* J1 nitrilase models into the negatively stained, three-dimensional electron microscopic reconstruction of the C-terminal truncated enzyme (Thuku et al., 2007). The left-handed spiral assembly is stabilized by two dyadic interactions located at the 'C' and 'D' surfaces. The principles of oligomerization along these surfaces are preserved in the microbial nitrilases. The subunits (rendered as ribbons), interact via the 'A' surface and this interface is conserved in the nitrilase superfamily (Pace and Brenner, 2001). Regions of vacant density in the 'C' surface correspond to the location of the insertions (not modeled). The figure was produced using UCSF Chimera (Pettersen et al., 2004).

**Table 1:** Characteristics of purified nitrilases, substrate specificity and enzyme activity

| Substrate Class | Organism | Substrate | % Relative activity or rate (U/mg or µmol/min) | Subunit (kDa) | Complex (kDa) | Amino Acids | Subunit | pH | Temp Opt °C | % Amide by-product | Reference |
|---|---|---|---|---|---|---|---|---|---|---|---|
| Aromatic | *Aspergillus niger K10* | Benzonitrile<br>4-cyanopyridine | 100<br>410.7 | 38.5 | >650 | 357 | Long helices | 8 | 45 | 84 of 2-picolinamide | Kaplan et al., 2006c; Vejvoda et al., 2008 |
| | *Arthrobacter* sp. strain J1 | Benzonitrile<br>*p*-Tolunitrile | 100<br>125 | 30 | 30 | ---- | 1 | 8.5 | 40 | ---- | Bandyopadhyay et al., 1986 |
| | *Geobacillus pallidus* Dac521 | Benzonitrile<br>Crotonitrile | 100<br>80.3 | 41 | 600 | 323 | 14 | 7.6 | 65 | ---- | Alamatawah et al., 1999 |
| | *Fusarium solani* IMI 196840 | Benzonitrile<br>Acrylonitrile | 100<br>6.6 | 76 | 620 | | 8 | 7.8-9.1 | | ---- | Harper ,1977a |
| | *Fusarium oxysporum* f.sp. *melonis* | Benzonitrile<br>Acrylonitrile | 100<br>35 | 37 | 550 | ---- | 14 | 6-11 | 40 | 4-6 of benzamide | Goldlust and Bohak, 1989 |
| | *Fusarium solani* O1 | Benzonitrile<br>4-cyanopyridine | 100<br>130 | ~40 | 580 | ---- | 14 | 8 | 40-45 | <1 of benzamide<br><3 isonicotinamide | Vejvoda et al., 2008 |
| | *Norcadia* (Rhodoccocus) NCIMB 11215 | Benzonitrile<br>*m*-nitrobenzonitrile | 100<br>841.7 | 45 | 560 | ---- | 12 | 7-9.5 | 30 | ---- | Harper, 1985 |
| | *Norcadia* (Rhodococcus) NCIMB 11216 | Benzonitrile<br>*m*-nitrobenzonitrile | 100<br>174.8 | 45.8 | 560 | ---- | 12 | 8 | 30 | ---- | Harper, 1977b<br>Hoyle et al., 1998 |
| | *Rhodococcus rhodochrous* ATCC 39484 | Benzonitrile<br>2-furancarbonnitrile | 100<br>171 | 40, 40.3 | 560 | ---- | 14 | 7.5 | 40 | 2 of phenyl acetamide | Stevenson et al., 1992 |
| | *Rhodococcus rhodochrous* J1 | Benzonitrile<br>Acrylonitrile | 100<br>128 | ~40 | 80, 410,<br>480, >1.5 MDa | 366 | 10, 12, long helices | 7.6 | 45 | 0.00022 benzamide | Kobayashi et al., 1989, Nagasawa et al., 2000; Thuku et al., 2007. |
| | *Rhodococcus rhodochrous* PA-34 | Benzonitrile<br>acrylonitrile | 100<br>22.4 | 45 | 45 | ---- | 1 | 7.5 | 35 | ---- | Bhalla et al., 1992 |
| Aliphatic | *Acidovorax facilis* 72W | Fumaronitrile<br>Benzonitrile | 100<br>4.6 | 40 | 570 | 369 | 14 | 8-9 | 65 | ---- | Gavagan et al., 1999; Chauhan et al., 2003 |
| | *Acinetobacter* sp. AK226 | Acrylonitrile<br>Racemic Ibu-CN<br>Benzonitrile | 144<br>100<br>94 | 41,43 | 580 | ---- | 14 | 8 | 50 | ---- | Yamamoto and Komatsu 1991 |
| | *Arabidopsis thaliana* AtNIT1 | 3-phenylpropionitrile<br>Benzonitrile | 729<br>2.7 | 38 | 450 | 346 | 12 | 9 | 35 | 95 of 3-nitroacrylamide | Osswald et al., 2002 |
| | *Bradyrhizopium japonicas* USD 110 (blr3397) | Hydrocinnamonitrile<br>Benzonitrile | 431<br>1 | 34.5 | ~340 | 321 | 10 | 7-8 | 45 | ---- | Zhu et al., 2008 |
| | *Comamonas testosteroni sp.* | Adiponitrile<br>Benzonitrile | 100<br>4 | 38,38.7 | ---- | 354 | ---- | 7 | 30 | | Levy-Schil et al., 1998 |
| | *Pseudomonas* sp. S1 | Acrylonitrile<br>Benzonitrile | 100<br>3.8 | 41 | 41 | ---- | ---- | ---- | ---- | ---- | Dhillon et al., 1999a, 1999b |
| | *Pyrococcus abyssi* | Malononitrile | 0.14 (U/mg) | 29.8 | 60 | 262 | 2 | 7.4 | 100 | ---- | Mueller et al., 2006 |
| | *Rhodococcus rhodochrous* K22 | Acrylonitrile<br>Benzonitrile | 348<br>27.1 | 41 | 650 | 383 | 14-16 | 5.5 | 50 | ---- | Kobayashi et al., 1990,1992 |
| | *Synechocystis* sp. strain PCC6803 | Fumaronitrile<br>Benzonitrile | 12000<br>100 | ~40 | 390 | 346 | 10 | 7 | 50 | ---- | Heinemann et al., 2003 |

| | | | | | | | | | | | |
|---|---|---|---|---|---|---|---|---|---|---|---|
| Bromoxynil-specific nitrilase | *Klebsiella pneumoniae* ssp. *ozaenae* | Bromoxynil<br>4-hydroxybenzonitrile | 15<br>0.23 (μmol/min/mg) | 37, 38.1 | 74 | 349 | 2 | 9.2 | 35 | ---- | Stalker et al., 1988 |
| Arylacetonitrilase | *Alcaligenes faecalis* ATCC 8750 | *p*-Aminobenzylcyanide<br>Benzonitrile | 1670<br>1.1 | 32 | 460 | ---- | 14 | 7.5 | 45 | ---- | Yamamoto et al., 1991, 1992. |
| | *Alcaligenes faecalis* JM3 | 2-thiopheneacetonitrile<br>*p*-Chlorobenzylcyanide | 100<br>188.7 | 38.9, 44 | 260, 275 | 356 | 6 | 7.5 | 45 | ---- | Nagasawa et al., 1990; Kobayashi et al., 1993 |
| | *Bradyrhizobium japonicus* USD110 | Phenylacetonitrile<br>Mandelonitrile | 100<br>460 | 37 | 455 | 334 | 12 | ---- | ---- | ---- | Zhu et al., 2007 |
| | *Pseudomonas fluorescens* DSM 7155 | Phenylacetonitrile<br>2-(Methoxy)-mandelonitrile | 100<br>10 | 38, 40 | 130 | ---- | 2 (or 3) | 9 | 55 | 3-5 of 2-(Methoxy)-mandelamide | Layh et al., 1998; Brady et al., 2004 |
| | *Pseudomonas fluorescens* EBC191 | 2-phenylvaleronitrile<br>Benzonitrile | 5600<br>0.25 | 37.7 | ---- | 350 | ---- | 6.5 | 50 | 43 with O-Acetylmandelonitrile | Kiziak et al, 2005 |
| Cyanide dihydratase | *Alcaligenes xylosoxidans* ssp. *denitrificans* strain DF3 | NaCN | 81 (μmol/min/mg) | 39,40 | >300 | ---- | ---- | 7.6-8.0 | 26 | ---- | Ingvorsen et al., 1991 |
| | *Bacillus pumilus* strains C1 and 8A3 | KCN | 97 (μmol/min/mg) | 37.3 | 672 | 330 | 18, 22, long helices | 7.8-8.0 | 37 | ---- | Jandhyala et al., 2003<br>Eicher J, *personal communication* |
| | *Pseudomonas stutzeri* AK61 | KCN | 54.6 (μmol/min/mg) | 38 | 532 | 334 | 14 | 7.5 | 30 | ---- | Watanabe et al., 1998; Sewell et al., 2003 |
| Cyanide hydratase | *Fusarium lateritium* | KCN<br>Benzonitrile | 100<br>0.033 | 43 | 1217 | 356 | ---- | 7.5 | ---- | 100 | Cluness et al., 1993; Nolan et al., 2003 |
| | *Fusarium solani* | KCN<br>$K_2Ni(CN)_4$,$K_4Fe(CN)_6$ | 1.7(μmol/min/mg) | 45 | >300 | 363 | ---- | 7.5 | 25 | 100 | Barclay et al., 1998; Barclay et al., 2002. |
| | *Fusarium oxysporum* N-10 | KCN<br>Benzonitrile | 233000<br>0 | 40 | 160 | ---- | 4 | 7.5 | 30 | 100 | Yanase et al., 2000 |
| | *Gloeoecercospora sorghi* | KCN | 555 (μmol/min/mg) | 45, 40.9 | >300,<br>2-10 MDa | 368 | Long helices | | | 100 | Fry and Munch 1975; Wang and Van Etten 1992b |

Note: The activity with benzonitrile was often found to be 100% except in those nitrilases that do not hydrolyze aromatic substrates at all. The % relative activity or activity rate (U/mg or μmol/min) is quoted directly from the referenced publications. Different units are used by the authors when reporting activity. In most cases, this was determined for various substrates by enzyme kinetic studies or the use of activity assays. The experimental conditions and methods are generally different for all cases reported to date.

**Table 2**. Summary of the modifications which produced significant effects on the characteristics of the native/recombinant microbial enzyme

| Organism | Modification | Effect | Comment | Reference |
|---|---|---|---|---|
| *Acidovorax facilis* 72W | T210A/I/C, L201Q, F168V+L201N<br>T210G<br>F168K/T/ L/T/V/M | Increased activity and specificity<br>inactive<br>increased activity, specificity and stability | L201 and T210 are located in α6<br>F168 is at the junction of the $3_{10}$ helix and α5 | Wu et al., 2007, 2008 |
| *Bacillus pumilus* C1 | 303stop, hybrid (residues 287 – end from *P. stutzeri*)<br>293stop<br>279stop, deletion 219-233, Y201A/A204D<br>90EAAKRNE96/90AAARKNK96 | Full activity<br><br>Reduced activity<br>Inactive<br>Full activity | Relatively insensitive to C-terminal truncation and modification.<br><br>C and A surface mutations cause loss of activity<br>D surface mutation is tolerated | Sewell et al., 2005 |
| *Fusarium lateritium* | T12Q, S13A, K136R, D276E, V281A, M302S<br>T12P<br>F170L<br>S13A + K136R or V281A<br>S13A+K136R+V281A+M302S<br>S13A+K136R+ D276E +V281A+M302S<br>All the above | Normal protein expression and reduced activity<br>Inactive<br>Normal expression, inactive and could not grow on nitriles as $N_2$ source<br>Low protein expression, reduced activity and stability<br>Poor protein expression and no activity<br>Reduced protein expression and activity<br>Low protein expression and no activity | T12 and S13 are at C-terminal side of β1<br>R136 occurs in the cyanide hydratases at this location in β5. | Nolan et al., 2003 |
| *Pseudomonas aeruginosa* (aliphatic amidase) | T103I<br><br>W138G<br><br><br>T103I + W138G | Reduced activity and stability compared to wild type, highly sensitive to urea inhibition, specific for aliphatic amides, optimum pH 6.5<br>Reduced activity, stability and sensitivity to urea inhibition compared to wild type, specific for aliphatic and aromatic amides, optimum pH 8.0-9.0<br>Reduced activity, stability and sensitivity to urea inhibition compared to wild type, specific for only aliphatic amides except acetamide, loss of activity with time, optimum pH 6.5 | T103 is adjacent to W144 and could have a role in positioning the loop containing E142.<br>W138 obstructs access to the active site pocket. | Karmali et al., 2001 |
| *Pseudomonas fluorescens* EBC191 | H296A/F/K/R<br><br>C-terminal deletion of 47-75 amino acids<br><br>Chimeric (tail swapped) enzymes | Reduced enzyme activity, stability and enantioselectivity, increased amide formation<br>Reduced enzyme activity, stability and enantioselectivity, and increased amide formation<br>Reduced activity and slight increase in amide formation | H296 is in an often conserved GHY sequence in the C-terminal region | Kiziak et al., 2007 |
| *Pseudomonas stutzeri* AK61 | Y53F<br>E104Q<br>E180Q, D247N<br><br>276stop, 285stop, 296stop, 302stop and 310stop<br>Y200D/C203D, deletion 220-234<br>Hybrid (residues 287-end from *B. pumilus*) | Reduced activity<br>Reduced activity, and loss of activity with time<br>No significant change in activity<br><br>Inactive<br>Inactive<br>Inactive | <br><br>Very sensitive to alteration or truncation of the C-terminal<br><br>200 and 203 are adjacent in α6 from two differnd monomers related by the two-fold axis. Insertion of like charges was intended to dirupt the interaction. | Watanabe et al., 1998<br><br><br>Sewell et al., 2005 |
| *Rhodococcus rhodochrous* J1 | 302 stop, 311stop<br>317 stop, 327stop, 340stop | Inactive<br>Active | Truncation at 327 leads to fibre formation | Thuku et al., 2007 |
| Unknown environmental isolate (Diversa nitrilase) | A55G, I60E, N111S, A190S/T, F191L/T/M/V, M199E<br>A190H<br>M199L | Increased enantioselectivity at low substrate concentration, slow reaction<br><br>Increased enantioselectivity at high substrate concentration, fast reaction<br>Increased enantioselectivity at high substrate concentration, slow reaction | The "enantio-selectivity hot-spots" at 190 and 191 are situated in the loop between β8 and α6. This region is difficult to model based on known homologues but probably forms a side of the opening to the active site. | DeSantis et al., 2003 |

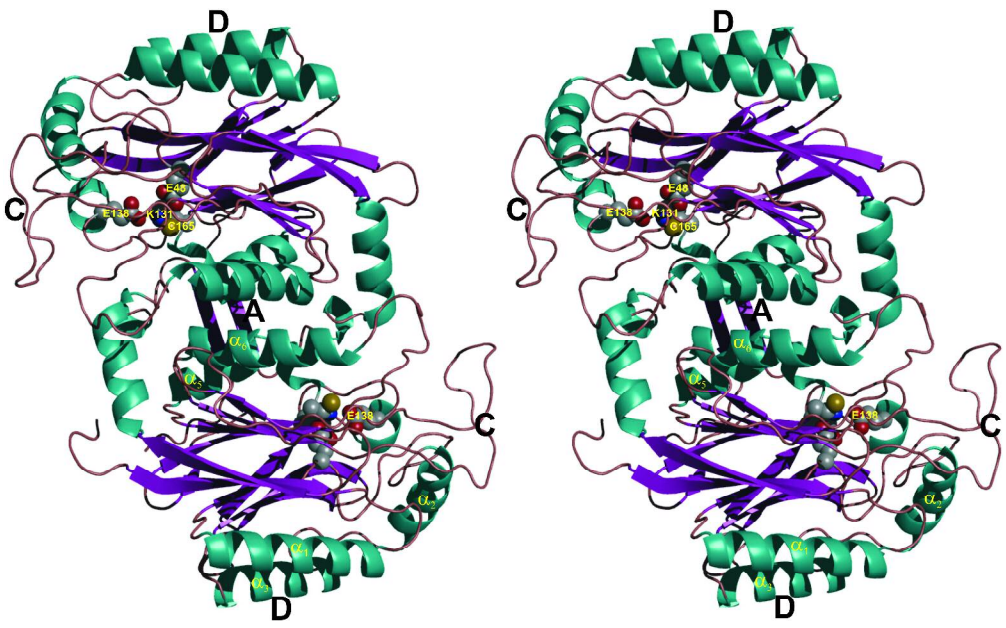


**Stereo view of a dimer model of the nitrilase from Rhodococccus rhodochrous J1. The model was built based on structural homology to the nitrilase-related atomic structures of 1erz, 1j31, 1ems and 2vhi (Nakai et al., 2000; Sakai et al., 2004, Pace et al., 2000 and Lundgren et al., 2008, respectively). The association surfaces are indicated in black. The conserved catalytic residues are shown as spheres. The alpha helices (α1, α3, α5 and α6) involved in the interacting surfaces are also highlighted. The figure was produced using PyMOL (DeLano, 2002).**

309x192mm (600 x 600 DPI)

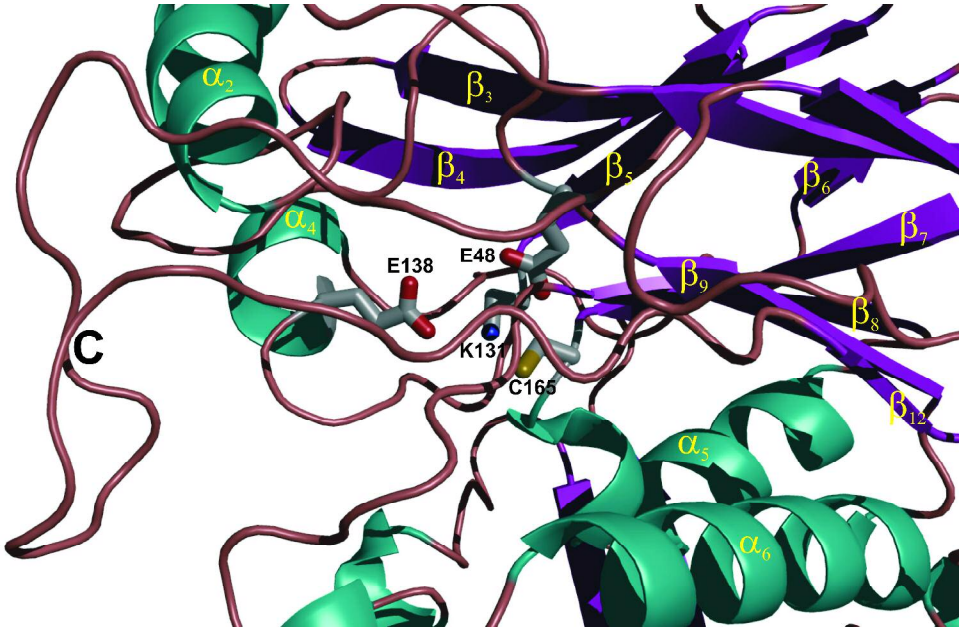


**A close-up view of the 'C' surface loop and the 'catalytic tetrad' in the active site of the model of the nitrilase from R.rhodochrous J1. The active site comprises a cysteine (C165), a lysine (K131), and two glutamates (E48 and E138). The location of E138 in a 'C' surface loop raises the possibility that association of dimers moves this residue (which corresponds to E142 in the amidase structure from Geobacillus pallidus (Kimani et al., 2007)) into the correct position for catalytic activity. The figure was produced using PyMOL (DeLano, 2002).**

209x130mm (600 x 600 DPI)

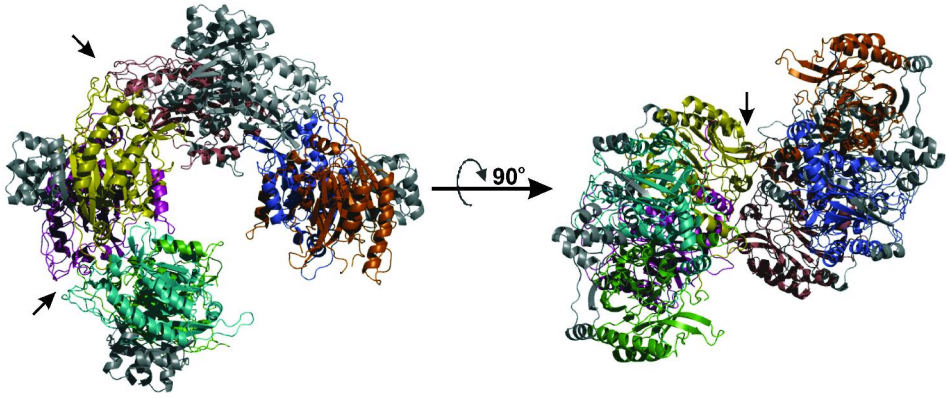


**Fig 2. The crystal structure of the nitrilase-related β-alanine synthase from Drosophila melanogaster (Lundgren et al., 2008). The association of the dimers occurs across the 'C' surface (black arrow) leading to a left-handed octameric assembly which does not close or complete a turn of the helix. The shape of the octamer appears similar to the 'c' shaped oligomers of the nitrilase from Rhodococcus rhodochrous J1 (Thuku et al., 2007). The fruit fly enzyme has an extended N-terminus (comprising 60-70 amino acids) which forms a four helical bundle (two from each subunit, grey) across the dimer interface. The C-terminus is located in the center of the spiral assembly. The figure was produced using PyMOL (DeLano, 2002).**
191x77mm (600 x 600 DPI)

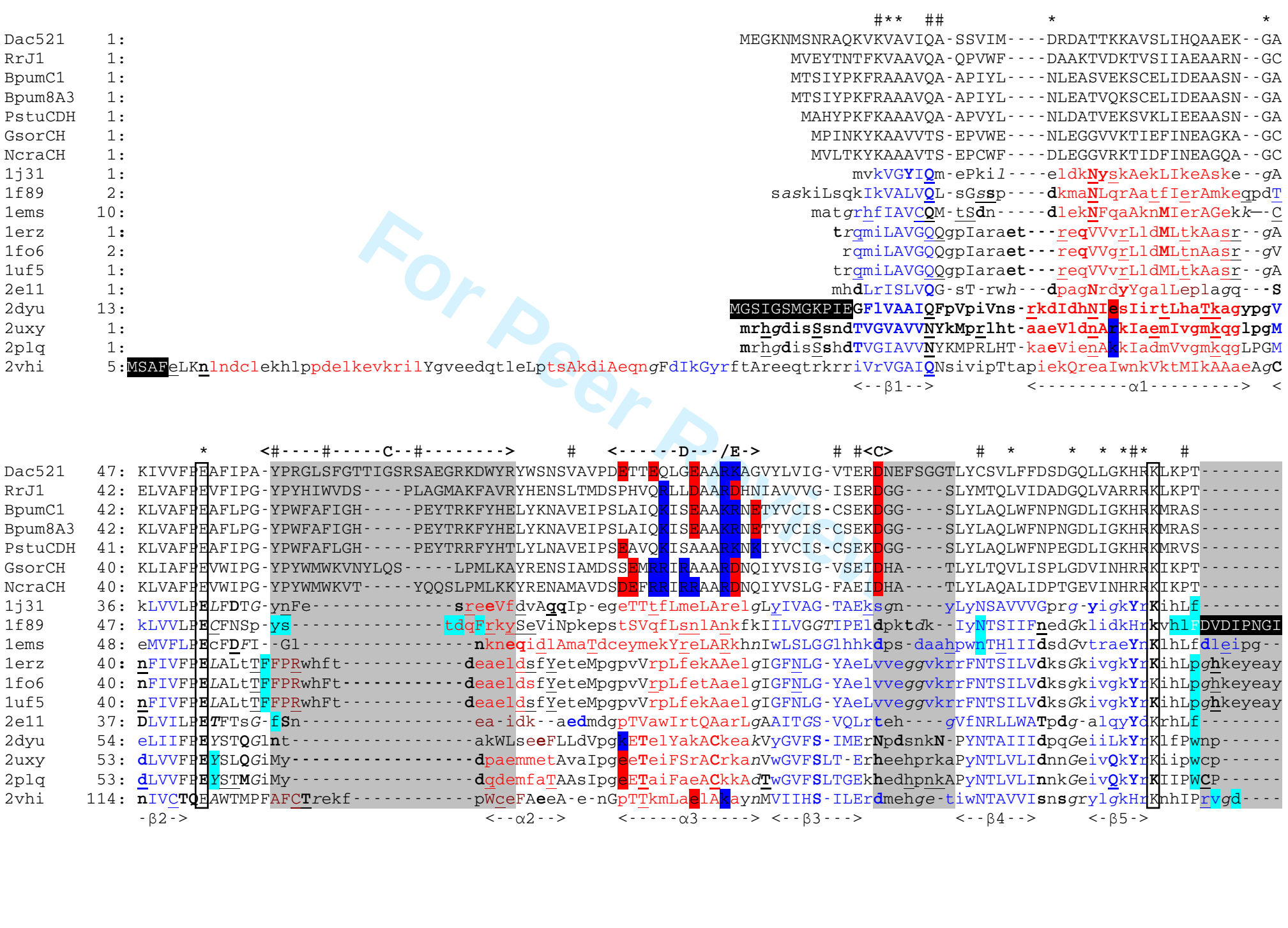

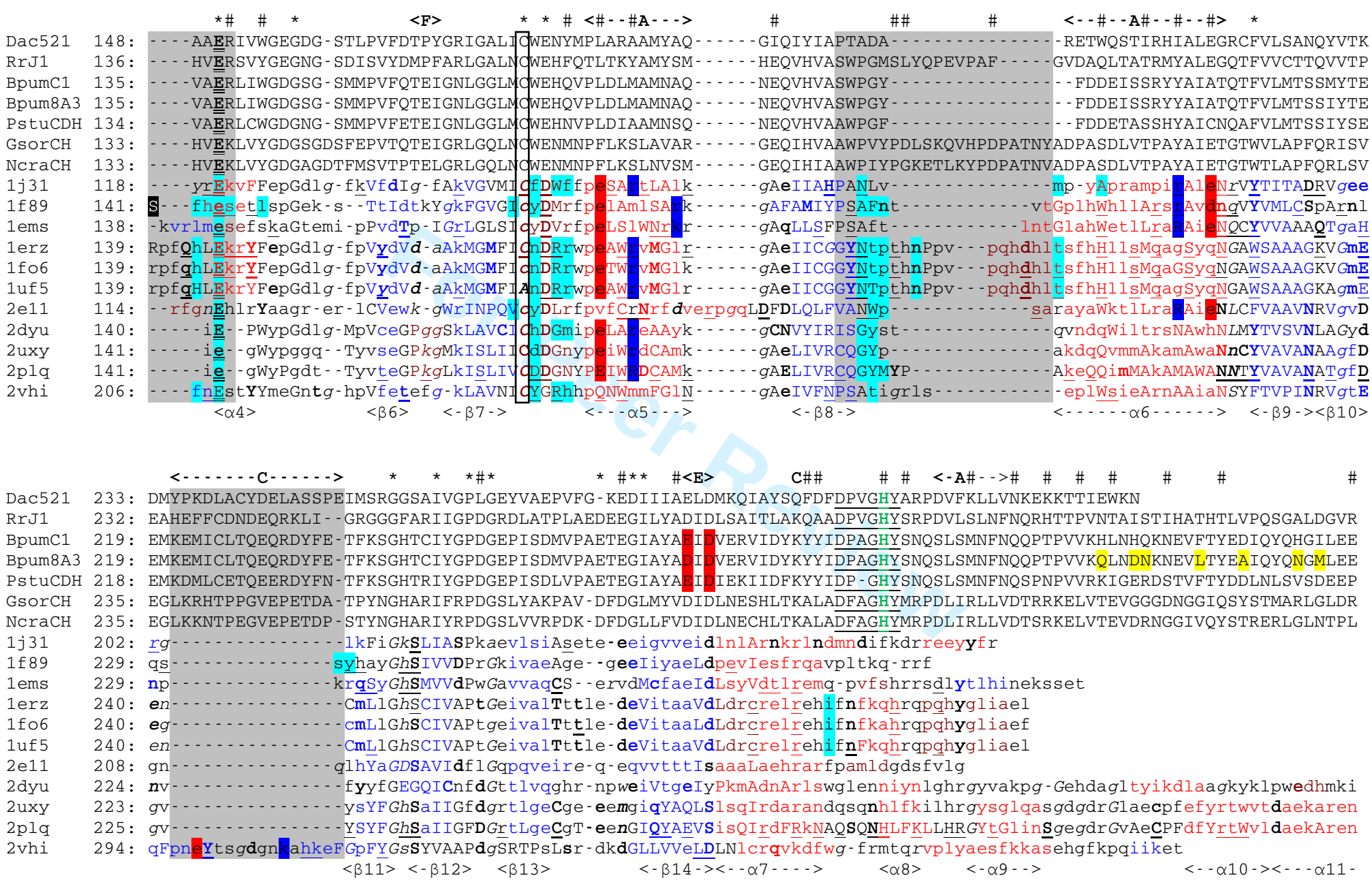
Dac521 148:
RrJ1 136:
BpumC1 135:
Bpum8A3 135:
PstuCDH 134:
GsorCH 133:
NcraCH 133:
1j31 118:
1f89 141:
1ems 138:
1erz 139:
1fo6 139:
1uf5 139:
2e11 114:
2dyu 140:
2uxy 141:
2plq 141:
2vhi 206:
<α4> <β6> <-β7-> <---α5---> <-β8-> <------α6------> <-β9-><β10>
Dac521 233:
RrJ1 232:
BpumC1 219:
Bpum8A3 219:
PstuCDH 218:
GsorCH 235:
NcraCH 235:
1j31 202:
1f89 229:
1ems 229:
1erz 240:
1fo6 240:
1uf5 240:
2e11 208:
2dyu 224:
2uxy 223:
2plq 225:
2vhi 294:
<β11> <-β12> <β13> <-β14-><--α7----> <α8> <-α9--> <--α10-><---α11-

```
RrJ1     341: ELNGADEQRALPSTHSDETDRATASI
BpumC1   329: KV
Bpum8A3  329: KV
PstuCDH  328: VVRSLRK
GsorCH   344: PLEEEDYRQGTDAGETEKASSNGHA
NcraCH   344: ENDKEGKK
2dyu     317: kdgsiygyptt-ggrfgk
2uxy     317: verltrsttGvaqcpvgrlpyegLEKEA
2plq     319: VekiTrstVGTaeCpiqgIpneGKTKEIGV
              --->
```

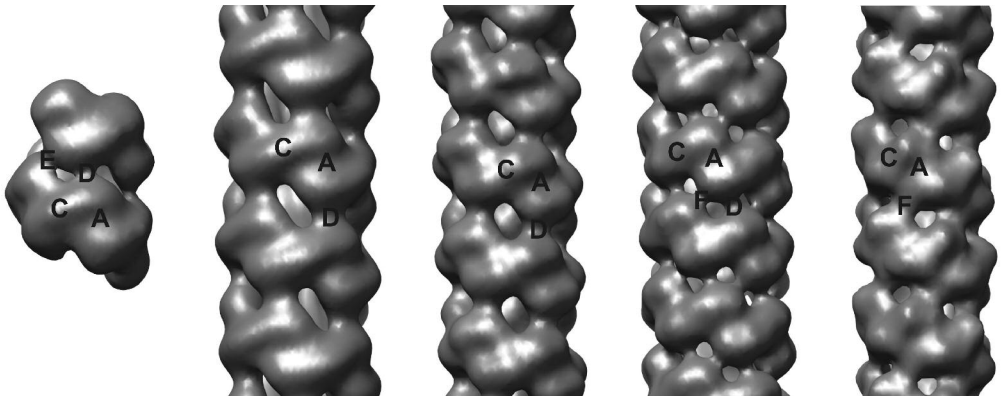


**Fig 4. Three dimensional electron microscopic reconstructions of the microbial nitrilases studied by us at low-resolution. These include (from left to right), the terminating 14-subunit spiral of the cyanide dihydratase from Pseudomonas stutzeri AK61 (Sewell et al., 2003), the variable length helices of the cyanide dihydratase from Bacillus pumilus C1 at pH 5.4 (Δϕ = -77o, Δz = 15 Å, Scheffer, 2006) and the C-terminal truncated nitrilase from Rhodococcus rhodochrous J1 (Δϕ = -73.5, Δz = 15.8 Å, Thuku et al., 2007), and the cyanide hydratases from Neurospora crassa ((Δϕ = -66.7o, Δz = 13.6 Å, Dent et al., 2008) and Gloecercospora sorghi ((Δϕ = 66o, Δz = 13 Å, Woodward et al., 2008), respectively. The shape of the dimer and the connectivity defining a left-handed one-start spiral can clearly be discerned. The 'A' surface is preserved in all members of the nitrilase superfamily. All structures conserve a two-fold axes at the dimer interface ( the 'A' surface) whose line passes through a hole on the other side of the spiral in the case of the nitrilase and cyanide dihydratases, or through the 'F' surface in the case of the fungal cyanide hydratases. A second dyad is found to occur at the 'C' surface with a line passing through the 'D' surface on the other side of the spiral. The 'E' surface is asymmetric and is found to occur specifically in the terminating spiral. The conservation of the insertions at the 'C' surface and the possibility of salt bridge formation across the groove of the helix (at either the 'D' or 'F' surface) suggest that spiral formation may be common among the microbial nitrilases. The figure was produced using UCSF Chimera (Pettersen et al., 2004).**

185x72mm (600 x 600 DPI)

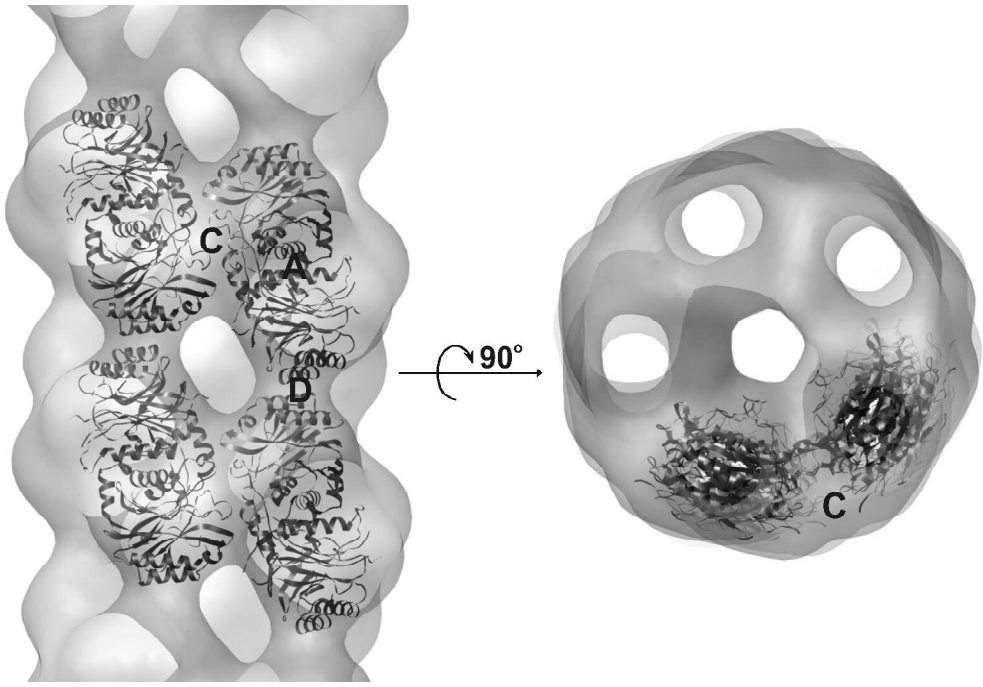


**The docking of Rhodococcus rhodochrous J1 nitrilase models into the negatively stained, three-dimensional electron microscopic reconstruction of the C-terminal truncated enzyme (Thuku et al., 2007). The left-handed spiral assembly is stabilized by two dyadic interactions located at the 'C' and 'D' surfaces. The principles of oligomerization along these surfaces are preserved in the microbial nitrilases. The subunits (rendered as ribbons), interact via the 'A' surface and this interface is conserved in the nitrilase superfamily (Pace and Brenner, 2001). Regions of vacant density in the 'C' surface correspond to the location of the insertions (not modeled). The figure was produced using UCSF Chimera (Pettersen et al., 2004).**

277x188mm (600 x 600 DPI)